

For Reference

NOT TO BE TAKEN FROM THIS ROOM

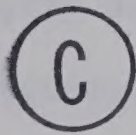
Ex LIBRIS
UNIVERSITATIS
ALBERTAEENSIS



THE UNIVERSITY OF ALBERTA

THE HALL EFFECT OF SILVER OXIDE

by



W.D. CARNE

A THESIS

SUBMITTED TO THE FACULTY OF GRADUATE STUDIES AND RESEARCH
IN PARTIAL FULFILMENT OF THE REQUIREMENTS FOR THE DEGREE
OF MASTER OF SCIENCE

DEPARTMENT OF ELECTRICAL ENGINEERING

EDMONTON, ALBERTA

FALL, 1971

UNIVERSITY OF ALBERTA

FACULTY OF GRADUATE STUDIES AND RESEARCH

The undersigned certify that they have read, and recommend to the Faculty of Graduate Studies and Research for acceptance, a thesis entitled "The Hall Effect of Silver Oxide" submitted by W.D. Carne in partial fulfilment of the requirements for the degree of Master of Science.

ABSTRACT

The Hall effect of sputtered thin films of silver oxide was observed at room temperature using an a.c. sample voltage and an a.c. magnetic field. The mobility was found to be about $0.05 \text{ cm}^2/\text{volt-second}$ for 3×10^6 ohm samples of Ag_2O with a band gap of 0.31 eV.

Although the silver oxide samples would decompose with time to Ag_2O , the films were relatively stable with the offset voltage of the samples varying only slightly with time. A high input impedance, low noise figure amplifier was designed and constructed using two junction FETs at the input. When used in combination with a band-pass filter, the offset voltage was reduced to a value below that of the noise voltage. Mobilities as low as $3 \times 10^{-3} \text{ cm}^2/\text{volt-second}$ could be detected using this arrangement. An improvement to the electronic circuit could have resulted in determining whether conduction was due to electrons or holes.

ACKNOWLEDGEMENTS

Appreciation is extended to those who assisted in the course of this research. In particular, the author is indebted to his supervisor Dr. C. G. Englefield for his overall advice and assistance. Acknowledgement must also be given to Mrs. V. Harwood for her assistance with the vacuum equipment, to Mr. E. M. Edwards for his assistance with the design of the electronic circuits, and to Dr. F. L. Weichmann of the Department of Physics who originated the project.

Many thanks are given to Mr. E. Buck and his staff for the many modifications made to the high vacuum unit. Gratitude is also expressed to the many graduate students for their time and help.

The author is further indebted to the National Research Council and the University of Alberta for financial assistance.

TABLE OF CONTENTS

	<u>Page</u>
1. Introduction	1
2. The Hall Effect	
2.1 Theory of the Hall Effect	3
2.2 Measurement of the Hall Effect	7
2.3 Applications of the Hall Effect	8
3. Preliminary Study of Silver Oxide	
3.1 Compressed Powder Samples	9
3.2 Sputtered Films	10
3.3 Equipment for Measurement of the Hall Effect	12
3.4 Measurement of the Hall Effect	13
4. Equipment Used in the Preparation of Silver Oxide Samples	
4.1 Introduction	15
4.2 C.V.C. High Vacuum Chamber	15
4.3 Edwards Microcircuit Jig	17
4.4 Masks	17
4.5 Glow Discharge Cleaning Ring	20
4.6 Cathodic Sputtering	21
4.7 Slide Cooling System	23

	<u>Page</u>
4.8 Thermocouple	24
4.9 Gas Mixing System	26
4.10 Air Admittance	27
4.11 Film Thickness Monitor	27
5. Preparation of Sputtered Silver Oxide Films	
5.1 Introduction	28
5.2 Determination of Slide Temperature	28
5.3 Determination of Optimum Sputtering Voltage and Pressure	31
5.4 Preparation of Low Resistance (Ohmic) Electrical Contacts	32
5.5 Effect of Sputtering Time	33
5.6 Effect of Gas Composition	34
5.7 Choice of Sample Position	34
6. Design of Electrical Equipment	
6.1 Methods of Measurement of the Hall Effect	36
6.2 Selection of Input Transistor for the Hall Voltage Amplifier	39
6.3 A.C. Voltage and Constant Magnetic Field	42
6.4 A.C. Voltage and Varying Magnetic Field	
6.4.1. Construction of an A.C. Magnet	44
6.4.2 The Sample Voltage Supply	46

	<u>Page</u>
6.4.3 The Hall Voltage Amplifier	
6.4.3.1 The Source Follower Amplifier	48
6.4.3.2 The Differential Amplifier	54
6.4.4 The Band-Pass-Rejection Filter	56
6.4.5 Performance of the Complete Circuit	62
7. Results	
7.1 Properties of Silver Oxide Films	64
7.2 Hall Effect Measurement	66
8. Conclusions	68
Bibliography	71
Appendix I Cathodic Sputtering	72
Appendix II Temperature Difference Across the Glass Slide While Sputtering	73
Appendix III Operational Amplifier	74

LIST OF TABLES

<u>Table</u>		<u>Page</u>
6.1	Thermal Noise Voltage versus Sample Resistance	40
7.1	Hall Voltage versus Time	66

LIST OF FIGURES

<u>Figure</u>	<u>Page</u>
2.1 Polarity of the Hall Voltage for an Electron Current	4
2.2 Polarity of the Hall Voltage for a Hole Current	4
2.3 Hall Sample Showing the Usual Contact Arrangement	7
3.1 Compressed Powder Silver Oxide Hall Sample	9
3.2 Sputtering Apparatus	11
3.3 Sputtered Silver Oxide Sample	12
3.4 Measuring Circuit for the Hall Effect	13
4.1 C.V.C. High Vacuum Chamber and Edwards Microcircuit Jig	16
4.2 Cross Section of Mask After Etching	18
4.3 Sample Mask	19
4.4 Shape of Hall Sample	20
4.5 Shape of Electrical Contacts	20
4.6 Cathode Arrangement	22
4.7 Cross Section of Metal Tubing	22
4.8 Cross Section of Sputtering High Voltage Line	22

<u>Figure</u>	<u>Page</u>
4.9 Slide Cooling Block	24
4.10 Top View of Cooling Block	25
4.11 Cross Section of Thermocouple	26
5.1 Ag-Ag ₂ O-AgO Phase Diagram	30
5.2 Relationships Between Voltage, Current, and Pressure	32
5.3 Mask for the Determination of Resistance versus Slide Position	35
5.4 Resistance versus Slide Position	35
6.1 Schematic Diagram of the Circuit for Constant Magnetic Field	43
6.2 Schematic Diagram of the Circuit for Varying Magnetic Field	43
6.3 Cross Section of a.c. Magnet	45
6.4 Schematic Diagram of Sample Voltage Supply	46
6.5 Drain Characteristics	48
6.6 Input Characteristics	48
6.7 Basic Source Follower	49
6.8 Complementary Compound FET Source Follower	50
6.9 Source Follower with Current Source	53
6.10 Hall Voltage Amplifier	55

<u>Figure</u>	<u>Page</u>
6.11 Band-Pass-Rejection Filter	57
6.12 Band-Pass Filter	57
6.13 Frequency Response of the Band-Pass Filter	59
6.14 Twin-T Rejection Filter and Amplifier	59
6.15 Frequency Response of the Band-Pass-Rejection Filter	
7.1 Variation of Sample Resistance with Time	65

1. Introduction

When a current passes through a conductor placed in a magnetic field, a voltage is produced between the sides of the conductor. Its magnitude is proportional to the magnitude of the current and to the strength of the magnetic field. This phenomenon is known as the Hall effect. It is used commercially in various applications where it can measure the strength of a magnetic field or even just to detect a magnetic field. The Hall effect is also used to determine the physical properties of a material such as its charge carrier concentration, the type of carrier, and the impurity atom concentration.

The investigation of the Hall effect of silver oxide (Ag_2O) was originally part of a study of the physical properties of silver oxide and its crystallographic analogue : cuprous oxide (Cu_2O). The study was being carried out on thin films of silver oxide which were sputtered in air. These films tended to decompose slowly with time. Measurement of the Hall voltage versus temperature would have yielded information about the mechanism of this decomposition. The Hall effect was to have been measured using a d.c. voltage amplifier circuit and other equipment that had been constructed to measure cuprous oxide. The amplifier proved to be inadequate due to the irregular decomposition rate of the sample, the long time constant of the amplifier, and the small Hall voltage.

Due to the technical problems which existed in the measurement of the Hall voltage, the project was transferred from the Department of Physics to the Department of Electrical Engineering. The stress of the project was changed from the study of the physical properties of silver oxide to the preparation of stable samples of silver oxide and to the design and construction of a low noise, high input impedance amplifier which would be able to measure a small Hall voltage. Measurements were then to be made of the Hall effect at room temperature.

2. The Hall Effect

2.1 Theory of the Hall Effect

When a current is passed through an electrically conducting material placed in a magnetic field, a voltage is produced between the sides of the conductor perpendicular to both the electric current and magnetic field. This phenomenon, the Hall effect¹ is caused by the Lorentz force which a magnetic field \vec{B} exerts on a moving charge. Electrons (or holes in the case of some semiconductor materials) are thus forced to one side of the sample. An electric field \vec{E} is formed by this concentration of electrons which will counterbalance the Lorentz force. This is shown in equation (2-1) for electron carriers

$$(\vec{B} \times \vec{v}) e = e \vec{E} \quad (2-1)$$

where \vec{v} is the velocity and e is the charge of an electron. If the current is in the x direction, and the magnetic field is in the z direction, then the Hall voltage will be in the y direction for an electron current.

$$\vec{E} = - \frac{1}{j} E_y = \frac{1}{j} e B_z v_x \quad (2-2)$$

This relation is shown in Figure 2.1 for an electron current and in Figure 2.2 for a (positive) hole current.

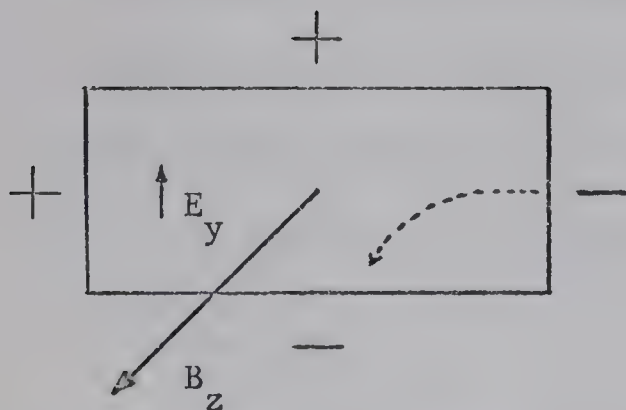


Figure 2.1 Polarity of the Hall Voltage for an Electron Current.

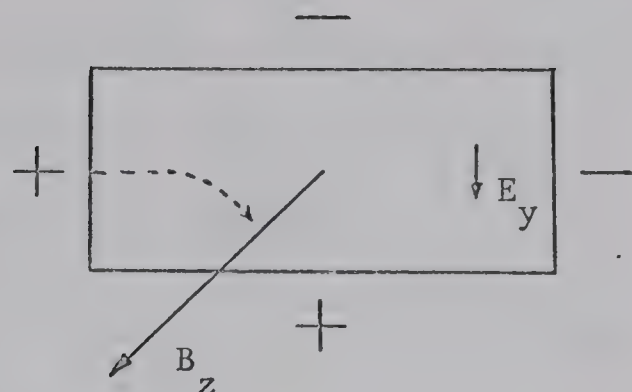


Figure 2.2 Polarity of the Hall Voltage for a Hole Current.

The electron current density \vec{J} is given by

$$\vec{J} = n e \vec{v} \quad (2-3)$$

where n is the free electron density. Equation (2-2) may be re-written as :

$$E_y = - B_z J_x / n e \quad (2-4)$$

$$E_y = R B_z J_x \quad (2-5)$$

where the Hall coefficient R is defined by :

$$R = - 1 / n e \quad (2-6)$$

For a hole current with a hole density p , the Hall coefficient is given by :

$$R = 1 / p e \quad (2-7)$$

From the magnitude of the Hall coefficient, the charge density

of the sample may be obtained. If the polarity of the Hall voltage is known, the sign of the Hall coefficient may be obtained, and from this the type (either electron or hole) of the majority carrier.

The electrical conductivity σ may be defined by :

$$J_x = \sigma E_x \quad (2-8)$$

The mobility μ is defined as :

$$\mu = v_x / E_x \quad (2-9)$$

Substituting equations (2-8) and (2-9) into equation (2-3) it is seen that the conductivity for electrons is given by :

$$\sigma = n e v_x / E_x \quad (2-10)$$

$$\sigma = n e \mu \quad (2-11)$$

From equation (2-11) it is seen that the mobility may be defined as :

$$\mu = \sigma |R| \quad (2-12)$$

where $|R|$ is the modulus of the Hall coefficient. (i.e. the equation is independent of the type of conduction.)

The Hall equation may be written in terms of quantities which are normally measured by combining equations (2-5), (2-8) and (2-12) such that

$$V_y = \mu B_z V_x \frac{W}{\ell} \quad (2-13)$$

or

$$V_H = 10^{-8} \mu B V_s \frac{w}{\ell} \quad (2-14)$$

where $V_y = V_H$ - Hall voltage

w - width of Hall sample

$V_x = V_s$ - sample voltage

ℓ - length of Hall sample

B - magnetic induction (gauss)

The importance of the mobility of a material in determining the size of the Hall voltage is seen. The other factors in the equation can be controlled by the researcher.

The theory above assumed that the material being studied is isotropic so that its properties do not depend upon the crystal orientation of the Hall sample. By taking a more detailed examination of the movement of electrons in the crystal, it has been found that

$$R = -\alpha / n e \quad (2-15)$$

where α depends upon the crystal structure, impurity density, etc. of the sample. A value of $\alpha = 1.18$ is obtained for spherical energy surfaces and $\alpha = 1.93$ for ionized impurity scattering. One type of mechanism will usually be more important in one temperature region than all others. By plotting the Hall coefficient R , mobility μ , conductivity σ , etc. versus temperature it is possible to gain insight into the internal and structural properties of the material being studied.

2.2 Measurement of the Hall Effect

A typical Hall sample is shown in Figure 2.3. The samples are usually 0.5 cm to 2 cm long and 0.1 cm thick. The voltage is applied to the sample contacts I and II and the Hall voltage is measured between contacts 2 and 4. Contacts 1 and 3 are used for measurement of the conductivity as contacts I and II are not usually ohmic. Due to a nonhomogeneous resistance in the sample and imperfect positioning of the contacts, a voltage will appear between the Hall contacts 2 and 4 when a voltage is applied to the sample contacts, even though the magnet is turned off. This offset voltage is usually larger than the Hall voltage and provision must be made to eliminate it.

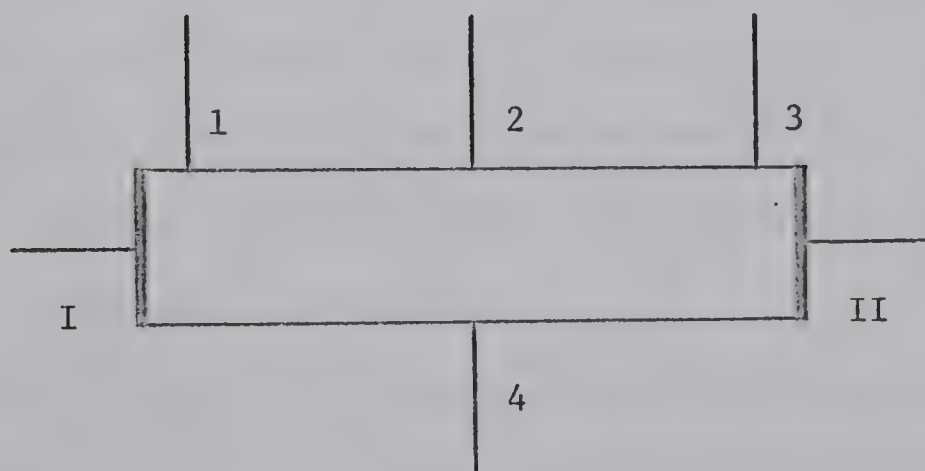


Figure 2.3 Hall Sample Showing the Usual
Contact Arrangement

Note that sample contacts I and II as shown in Figure 2.3 form a short circuit across the width of the Hall sample. If the distance between contacts I and II is less than four times the distance between the Hall contacts, then the Hall voltage will be partially shorted out.

2.3 Applications of the Hall Effect

One important application of the Hall effect is as a fluxmeter for measuring the strength of magnetic fields. Hall samples made from materials such as indium antimonide (Hall mobility : $100,000 \text{ cm}^2/\text{volt-second}$) are able to measure fields as small as 10^{-4} gauss so that very sensitive magnetometers can be built. Ion currents have been measured without disturbing the plasma by measuring the magnetic field associated with the current. By making the Hall effect probe very small, the uniformity of a magnetic field may be determined.

The Hall effect is also used as a sensor to locate the position of small magnets in such applications as positioning contactors in elevators, counting shaft rotations, and controlling read-write head positions in magnetic tape systems.

The Hall voltage is a product of applied voltage and applied magnetic field so that the effect may be used as a multiplier. Analogue multipliers with a linearity of 0.1% have been produced. Because the effect is independent of frequency, microwave wattmeters can also be built.

3. Preliminary Study of Silver Oxide

3.1 Compressed Powder Samples

Compressed powder samples of commercial grade silver oxide (Figure 3.1) were used in order to work with as low a resistance as possible. The procedure for preparing primitive samples involved placing a strip of silver oxide powder (2 cm. x 0.4 cm. x 0.1 cm.) on the 1.5" diameter piston of the press, placing wire leads in the sample, covering the piston with a 0.4 cm. layer of acetate powder ($\rho=10^{15}$ ohms-cm.) and compressing the entire assembly under a high pressure of 34,000 psig. The acetate gave strong mechanical support to the compressed powder and electrical leads. Ohmic electrical contacts were not obtained to the silver oxide powder.

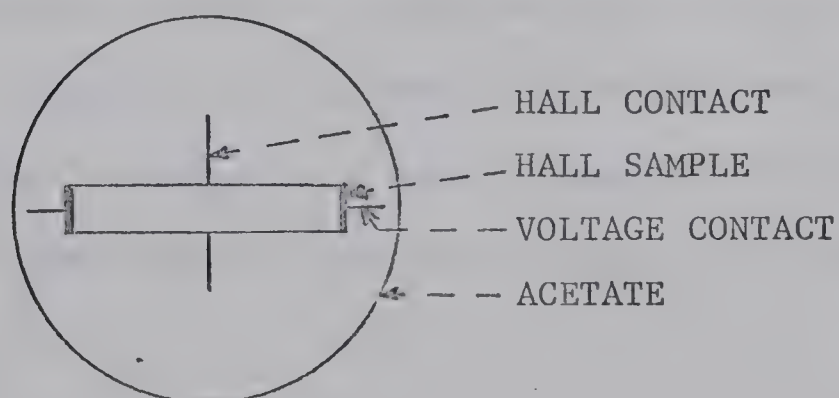


Figure 3.1 Compressed Powder Silver Oxide Hall Sample

Sample resistances of the order of 10^8 ohms were obtained at room temperature. It was found that the sample resistance did not change as the sample temperature changed - i.e. the powdered samples did not behave like a semiconductor. This could either have been due to interference between the silver oxide and the acetate background, to too high an impurity concentration conduction in the silver oxide, or to conduction along the boundaries of the powder. (The resistivity of 10^6 ohm-cm. was lower than the value for pure silver oxide of 10^7 to 10^8 ohms-cm.). Since powdered silver oxide did not provide good samples, studies of sputtered films (Appendix I) of silver oxide hence commenced.

3.2 Sputtered Films

Thin film samples of silver oxide had been produced in the Department of Physics using the apparatus shown in Figure 3.2. Sputtering conditions were 2000 V peak (half-wave rectified power supply), 8 mA current (0.5 mA/cm^2) and 0.15 torr oxygen pressure. The cathode to anode separation was about one inch. Sputtering time ranged from one to three hours. The sample substrate was placed on the anode which was cooled with liquid nitrogen in order to prevent the silver oxide samples from decomposing while under vacuum.

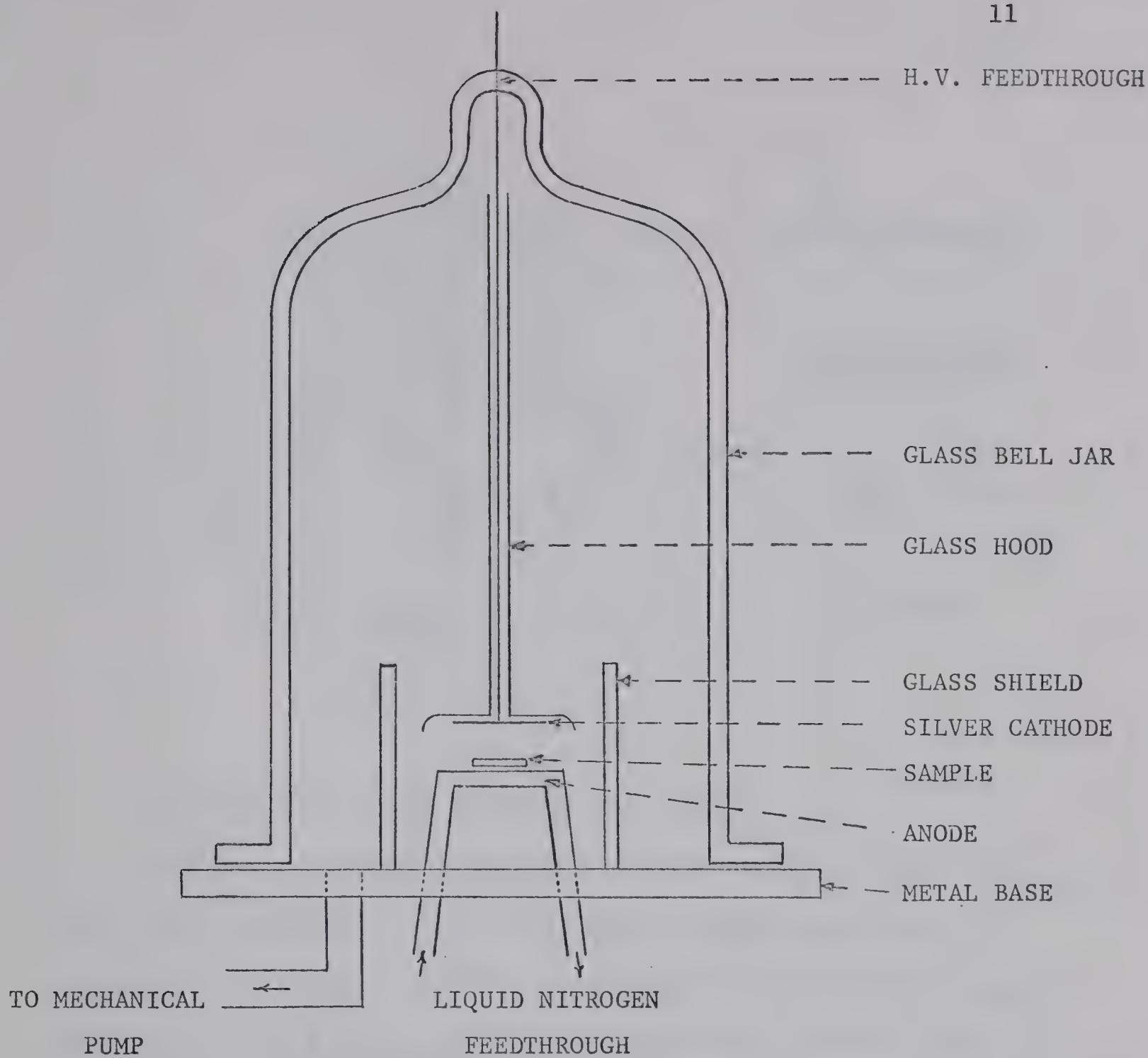


Figure 3.2 Sputtering Apparatus

Holes were made in beryllium oxide substrates and either aluminum or platinum wire contacts were mechanically attached. After the whole substrate had been sputtered, the excess silver oxide was removed leaving a sample approximately 1 cm x 0.2 cm (Figure 3.3).

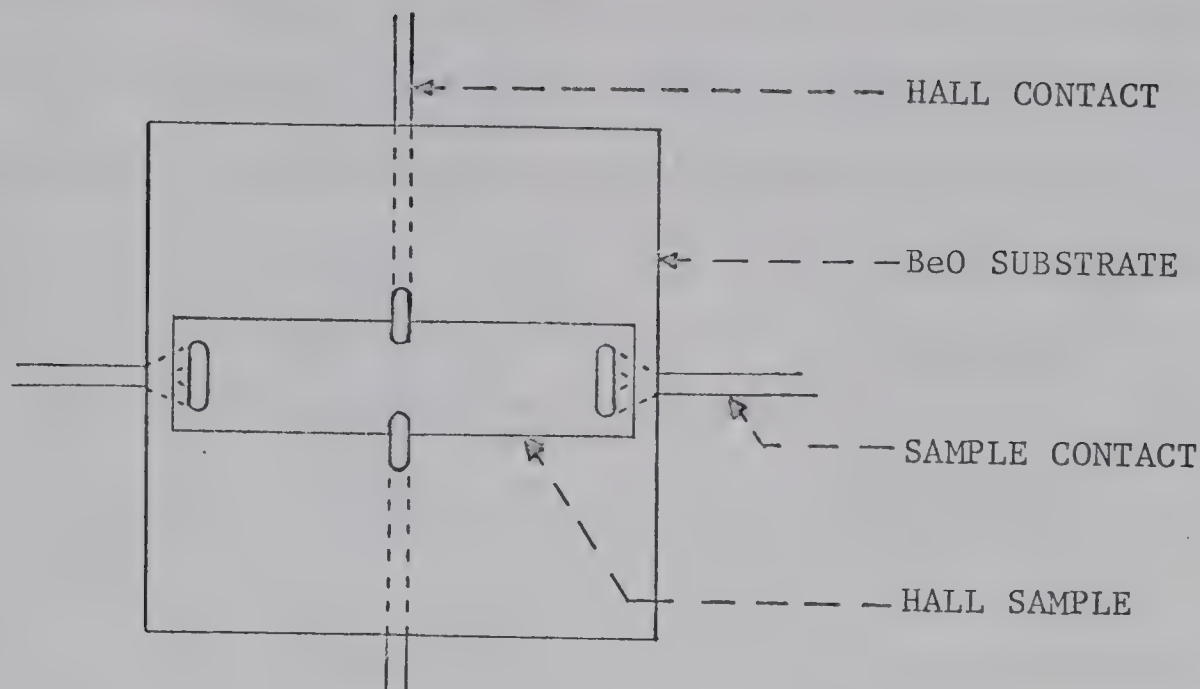


Figure 3.3 Sputtered Silver Oxide Sample

The initial sample resistance was typically 10^6 ohms to 10^9 ohms. The resistance increased slowly at room temperature over the period of a month to 10^{11} ohms (intrinsic silver oxide : Ag_2O). The samples would decompose rapidly above 90°C to 105°C with one atmosphere of oxygen pressure and become a greyish white color. The samples were initially opaque and dark brown but turned transparent amber when the resistance rose above 10^9 ohms. The films also became photoconductive above a resistance of 10^9 ohms.

3.3 Equipment for Measurement of the Hall Effect

Equipment to measure the Hall effect of cuprous oxide Cu_2O , which had a sample resistance of 10^9 ohms at room temperature, had been constructed in the Department of Physics. This equipment was

used to try to measure the Hall effect of silver oxide. A schematic diagram of the electrical circuit is shown in Figure 3.4. The Carey vibrating reed electrometer had an input impedance of up to 10^{15} ohms.

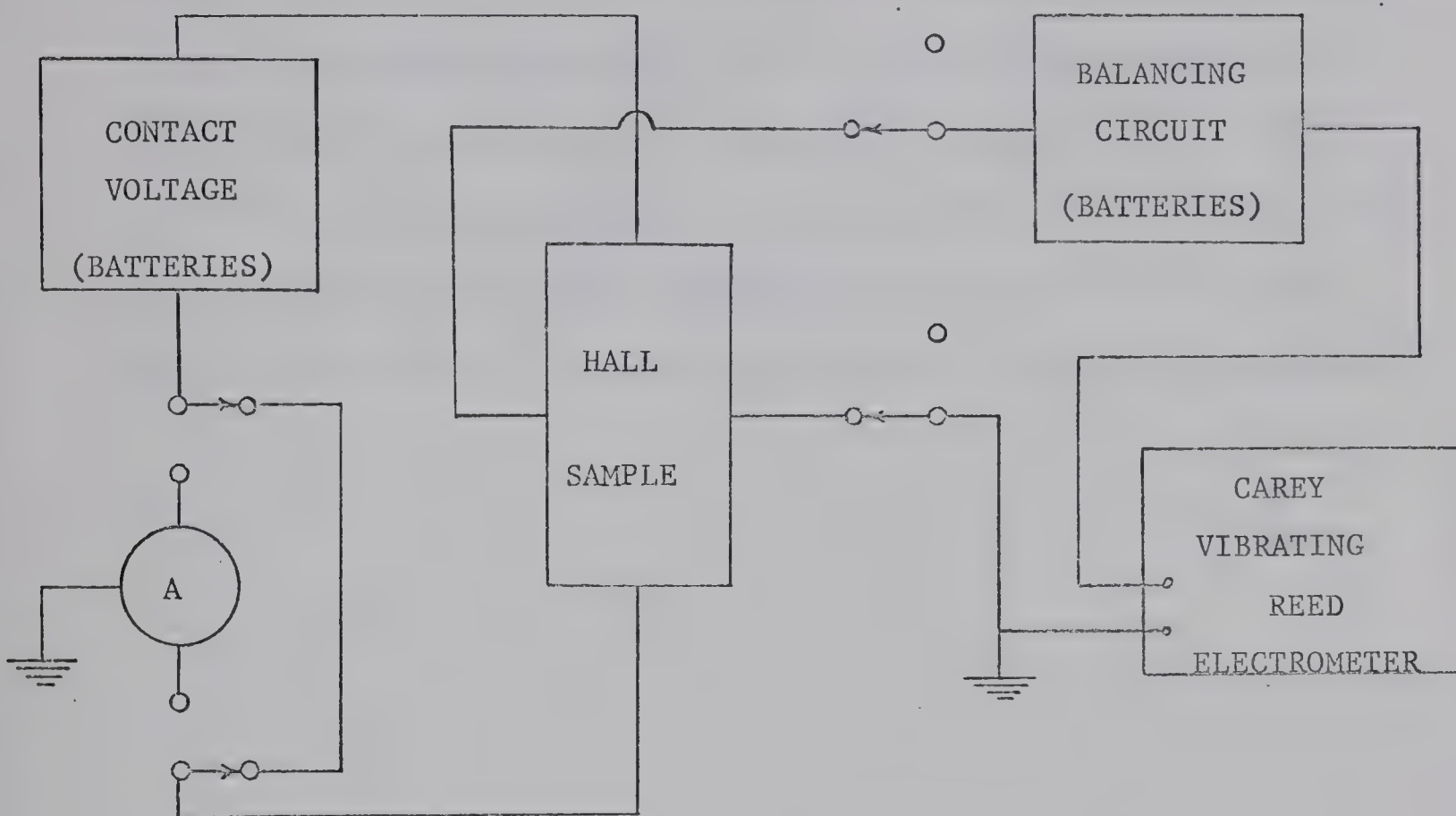


Figure 3.4 Measuring Circuit for the Hall Effect

When measuring the Hall voltage, the ammeter was disconnected. Similarly when measuring the current, the electrometer was disconnected. Both the Contact Voltage and the Balancing Circuit consisted of batteries which were insulated from ground. A constant magnetic field of 10,000 gauss (1 weber/m^2) was used.

3.4 Measurement of the Hall Effect

The circuit proved to be unsuitable for measurement of the Hall effect of silver oxide. The offset voltage drifted rapidly at about one percent of the applied voltage per minute caused by the

uneven decomposition of the silver oxide. It was thus impossible to balance the offset voltage to zero. The drift rate of the offset voltage decreased as the sample resistance approached 10^{11} ohms. Capacitance in the circuit gave a time constant of ten minutes at this high resistance. A 10 mV noise voltage was present. (The cuprous oxide samples by comparison had very little drift and a Hall voltage of about 1 V.) It could only be concluded from these tests that the Hall voltage was less than 10 mV and thus the mobility of silver oxide films was less than $1 \text{ cm}^2/\text{volt-second}$.

4. Equipment Used in the Preparation of Silver Oxide Samples

4.1 Introduction

The Vacuum Coating Unit which was used to prepare Hall effect samples in the Department of Electrical Engineering consisted of a Consolidated Vacuum Corp. (C.V.C.) High Vacuum Chamber containing an Edwards Microcircuit Jig (Figure 4.1). Modifications were made to permit cathodic sputtering and liquid nitrogen cooling of the sample. Production of thin film samples of precise geometry with a high degree of control of the sputtering parameters was possible. Reproducible Hall effect films were able to be sputtered.

4.2 C.V.C. High Vacuum Chamber

The C.V.C. High Vacuum Chamber (Figure 4.1) consisted basically of a six inch silicone oil diffusion pump and an eighteen inch (18") I.D. by three foot high glass bell jar. Modifications were necessary in order to install the microcircuit jig. A twenty inch I.D. steel cylinder and a one foot high bell jar were substituted for the larger glass bell jar. A molecular sieve trap at the input of the mechanical pump reduced contamination of the bell jar vacuum system with oil from the mechanical pump. A liquid nitrogen cooled chevron type baffle was used to prevent contamination of the bell jar vacuum system with oil from the diffusion pump and to reduce the ultimate vacuum pressure.

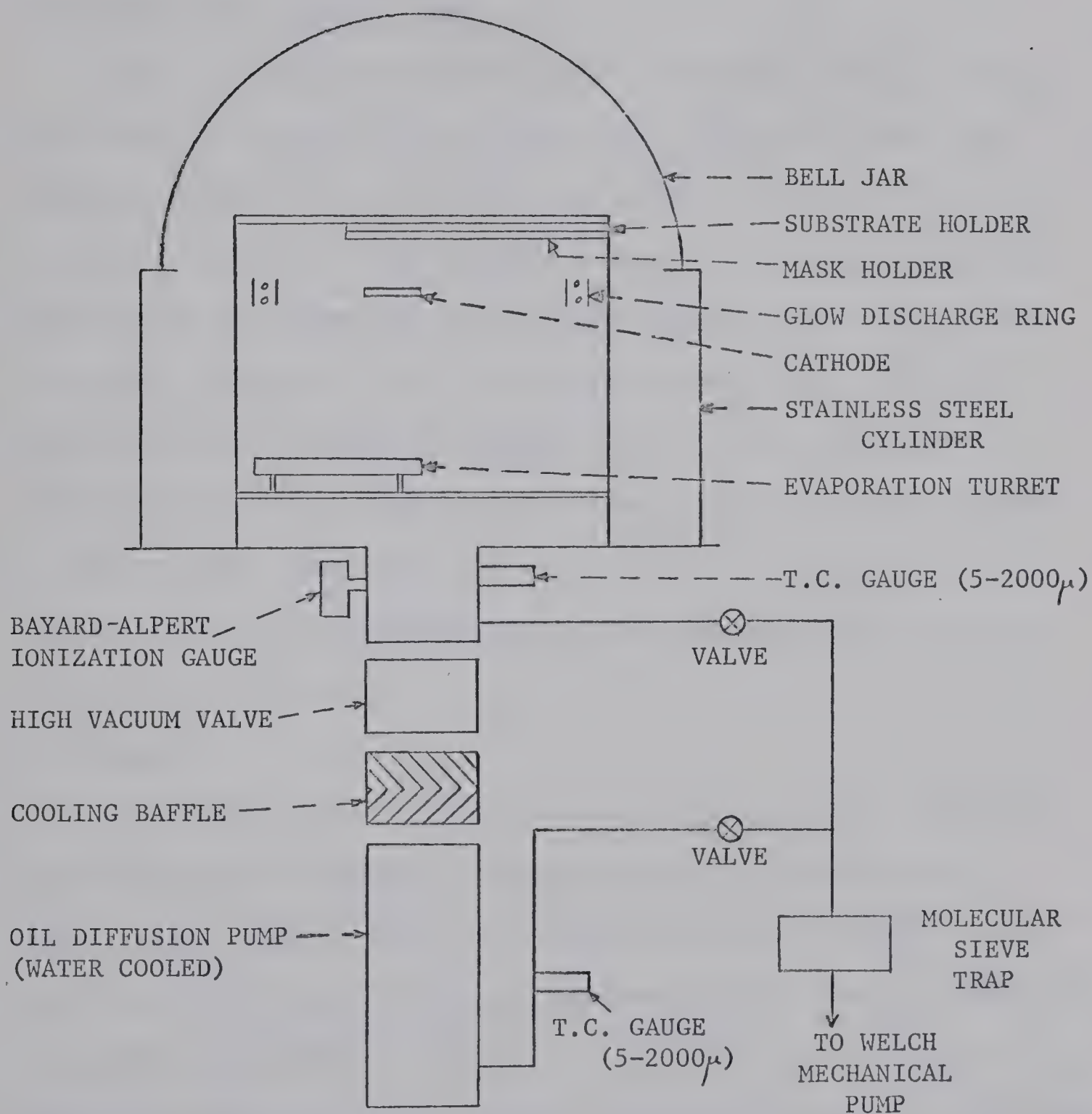


Figure 4.1 C.V.C. High Vacuum Chamber and Edwards Microcircuit Jig

Feedthroughs were available to pass high voltages, large currents, liquid nitrogen, etc. into the working system while it was under vacuum.

4.3 Edwards Microcircuit Jig

The C.V.C. High Vacuum Chamber was adapted in order to install the Edwards Microcircuit Jig (Figure 4.1). The microcircuit jig permitted evaporation of six different metals in any sequence onto as many as six 2" x 2" glass slides, using a predetermined sequence of up to six different masks. The masks could be positioned within an accuracy of 0.001". The slide magazines, the masks, and the evaporation sources could be rotated into position by means of external handwheels so that successive evaporations could be performed in sequence while under high vacuum conditions. Contamination of the samples was thus minimized and considerable time was saved in pumping the system out.

4.4 Masks

The masks used in the microcircuit jig were made of 0.002 inch thick sheets of molybdenum, a metal which sputters very poorly. Thicker masks (0.005") could not be used since they resulted in the edge of the Hall sample being much thinner than the center, caused by the shielding effect of the edge of the mask. A 0.005" thick molybdenum plate was needed to provide mechanical support to the thinner material in order to keep it firmly pressed against the glass slide.

The masks were produced by photoetching using Kodak Metal Etch Resist (KMER) and concentrated sulfuric acid. It was found that only thin coatings of resist would adhere to the molybdenum sheet during the developing process. The acid would eat through these thin coatings & it was necessary to add a heavy layer of KMER resist onto the sheet after the thin coat was developed. Precautions were needed as the KMER resist was very sensitive to light. Unless the KMER resist was kept in complete darkness after developing, a thin film of resist would cover the areas to be etched. This increased the etching time and thus increased the possibility of the acid softening the resist and causing it to peel off.

To keep the thickness of the Hall samples as even as possible, it was best to etch from the side of the mask which would be away from the glass slide during sputtering, as the etching process left a V-shaped cut as shown in Figure 4.2.

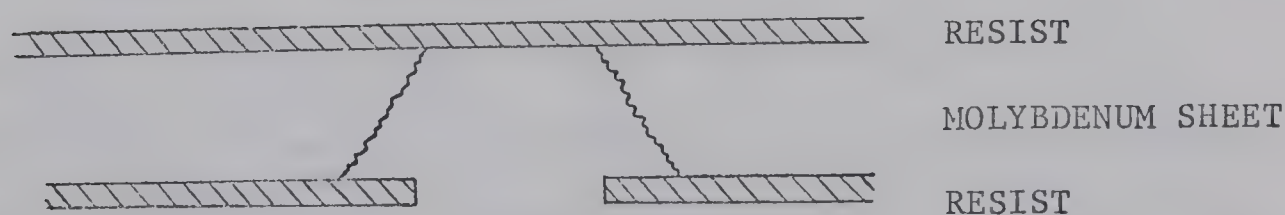


Figure 4.2 Cross Section of Mask after Etching.

The sample mask is shown in Figure 4.3 giving the position of the two Hall samples and the outline of the mask. The position of the Hall samples on the mask was chosen so as to be in areas of minimum resistance as is outlined in section 5.7. The circular holes are used for positioning the mask accurately in the mask holder of the microcircuit jig. The large circle in the mask exposed the thermocouple to the sputtering.

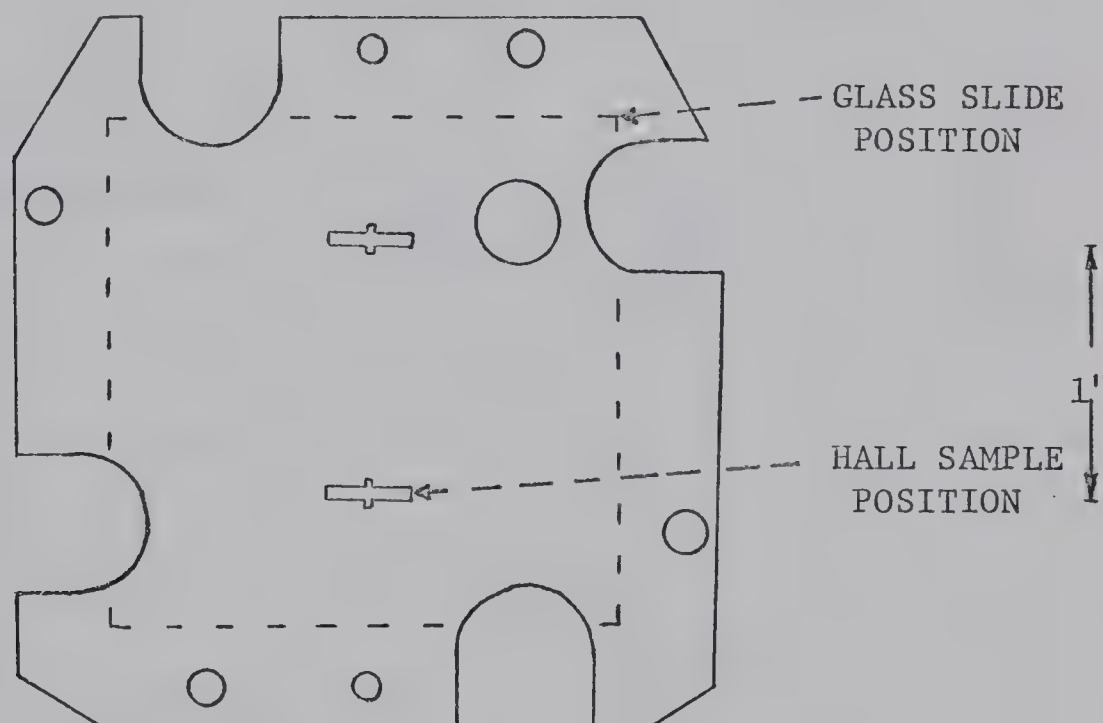
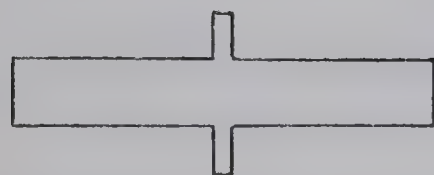


Figure 4.3 Sample Mask

The shape of the Hall sample and the shape of the electrical contacts are shown in Figure 4.4 and Figure 4.5 respectively. Contacts I and II were used to apply the voltage to the sample. Contacts 2 and 4 were used to measure the Hall voltage. They overlapped the "knobs" in the middle of the Hall sample. Contacts 1 and 3 were used to make

the conductivity measurements as the contact formed at I and II is usually non-ohmic. The distance between contacts 1 and 3 (0.2 in.) was four times the width of the Hall sample (0.05 in) so that the Hall signal was not shorted out.



0.1"

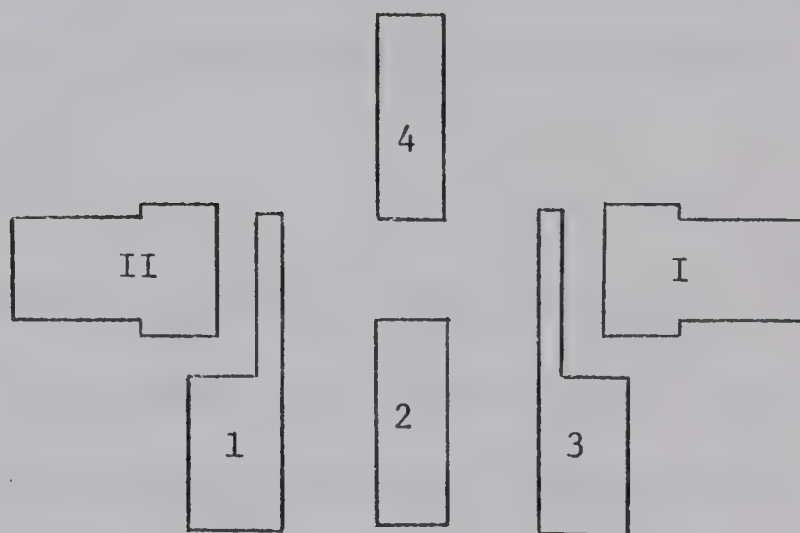


Figure 4.4

Shape of Hall Sample

Figure 4.5

Shape of Electrical Contacts

4.5 Glow Discharge Cleaning Ring

One of the accessories of the microcircuit jig was a glow discharge cleaning ring assembly (Figure 4.1). It consisted of two electrically isolated, pure aluminum rings about one inch apart. Glow discharge cleaning using argon gas was carried out at 30 μ

(0.03 mm. of mercury) with a voltage of 2000 V and a current of 10 mA. Higher voltages and currents resulted in overheating of the cathode aluminum ring. Use of the glow discharge cleaning lowered the ultimate pressure of the vacuum system to 5×10^{-7} torr.

Glow discharge cleaning could not be used during sputtering because the cathode would shield the glass slide from the glow discharge. After each sputtering, the silver oxide was cleaned off the microcircuit jig and cathode by dissolving the silver oxide in an ammonia solution.

4.6 Cathodic Sputtering

The microcircuit was modified to permit cathodic (diode) sputtering. The mask and slide holder were used as the anode. An aluminum cathode of three inch diameter was installed (Figure 4.6) 2" below the slide holder. A circular disk of the material to be sputtered was placed on top of the cathode. The cathode could either be placed directly below the glass slide or rotated to the side in order to evaporate. The cathode was electrically insulated from ground. The high voltage line to the cathode was enclosed in aluminum tubing (Figure 4.7 and Figure 4.8) to prevent glow discharge in the system. A cylindrical hood was placed on the cathode shield in order to limit contamination of the system while sputtering.

As approximately half the power used in sputtering was dissipated in the cathode, the aluminum cathode was water cooled. Cooling the cathode prevented possible decomposition of the silver oxide sample

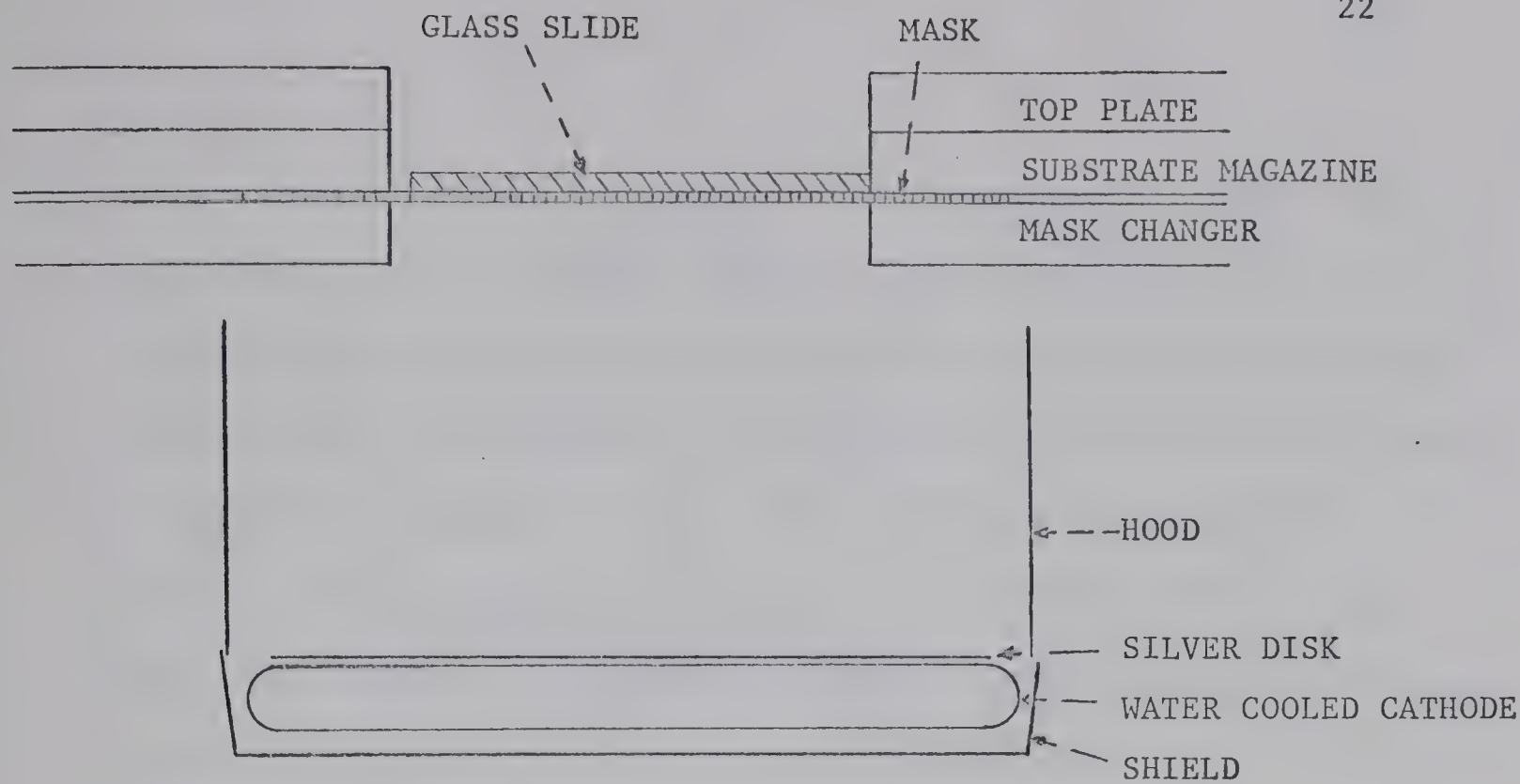


Figure 4.6 Cathode Arrangement

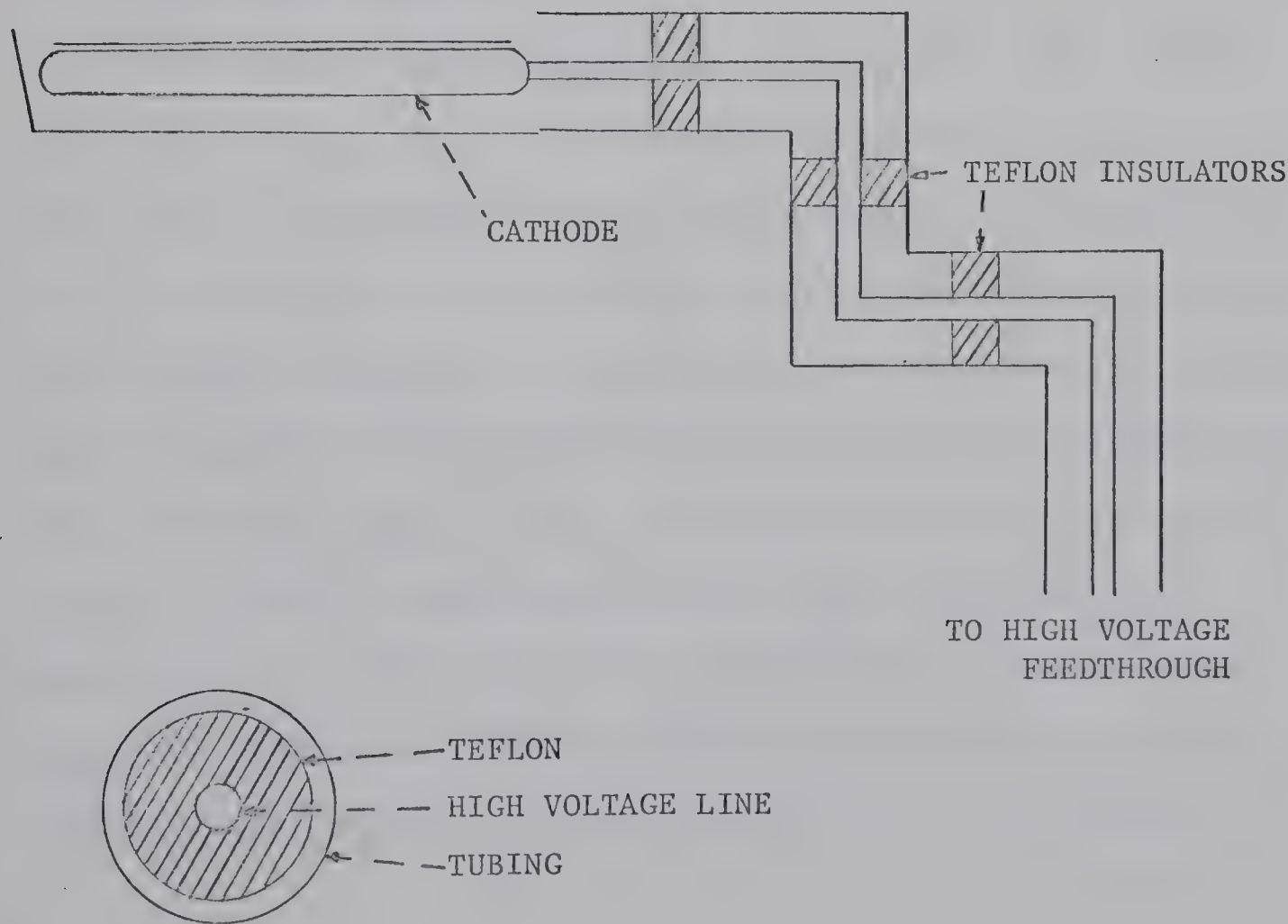


Figure 4.7 Cross Section of Metal Tubing

Figure 4.8 Cross Section of Sputtering High Voltage Line

by heat radiation from the cathode. The formation of silver oxide on the water cooled cathode, however, reduced the sputtering rate. Teflon tubing was used to make the connection from the coaxial water feedthrough to the cathode in order to provide the flexibility needed to permit the cathode to rotate. The teflon was wrapped with aluminum foil to prevent decomposition of the teflon during glow discharge cleaning. No detectable leakage current flowed through the water lines when the high voltage was applied.

A C.V.C. LC-031 power supply with the positive terminal at ground was used. For safety, a pressure switch was installed which caused it to automatically shut off whenever the system pressure rose above 100 torr.

4.7 Slide Cooling System

Silver oxide would decompose in vacuum unless cooled while sputtering. A copper cooling block (2" x 2" x 1½") (Figure 4.9) was constructed and rested flush on top of the glass slide using the port in the microcircuit jig normally used for the substrate heater. The block was clamped down to prevent it from being disturbed when the bell jar was lowered and to provide better contact with the glass slide. Only one sample could be made while the system was under vacuum as it was no longer possible to rotate the slide holder. Copper tubing was used to carry the cooling fluid, usually liquid nitrogen, between the coaxial feedthrough and the cooling block. Vertical travel of the block was limited to one to two inches.

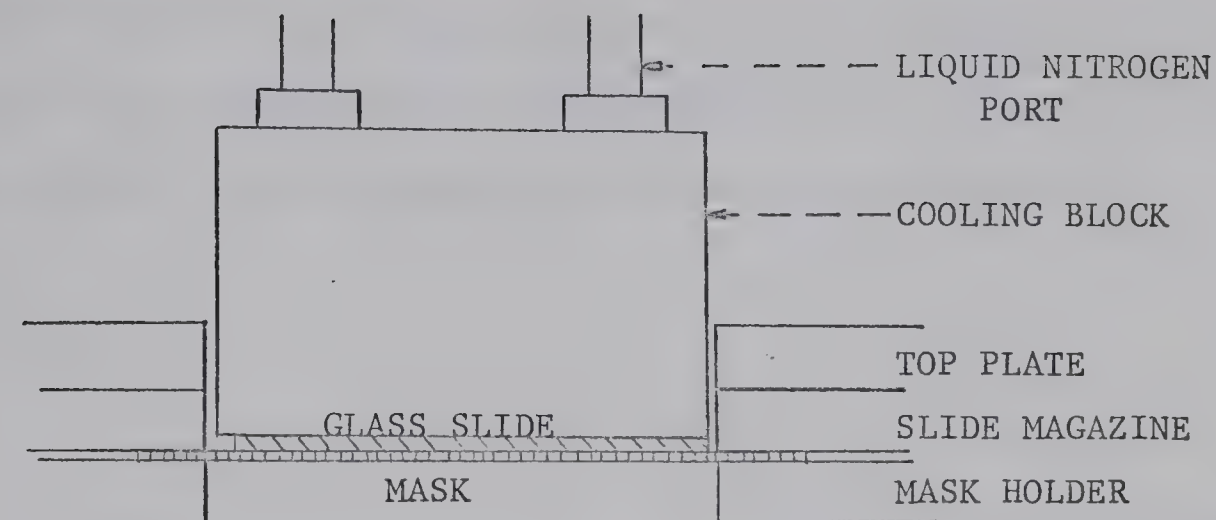


Figure 4.9 Slide Cooling Block

Compression fittings provided the seal between the tubing and the cooling block.

Liquid nitrogen was supplied from a 50 litre dewar which was pressured up to 30 psig. The cooling system would take two to four minutes to cool to the point that liquid nitrogen would come out the exit port. After sputtering had been completed, the system was warmed by passing compressed air through the cooling system. It took fifteen to twenty minutes to raise the temperature above the dew point and thus prevent condensation of water vapor on the sample.

4.8 Thermocouple

A thermocouple was required to measure the temperature of the glass slide while sputtering. Even though the copper block was milled flat, there was still poor thermal contact with the glass slide. The temperature difference between the top and bottom sides of the glass

slide should only be about one degree Centigrade (Appendix II) so that little error resulted in measuring the top surface of the glass. A quarter inch diameter hole was provided at the edge of the cooling block (Figure 4.10) in which the thermocouple was placed.

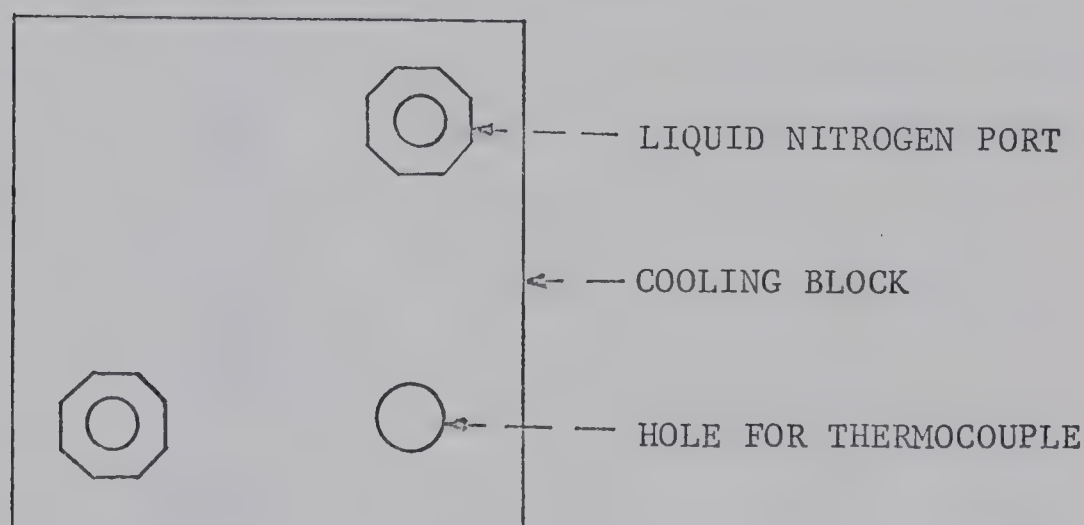


Figure 4.10 Top View of Cooling Block

Several designs of thermocouple support were tested, but most suffered from thermal contact problems with the cooling block. The thermocouple shown in Figure 4.11 provided the most accurate measurements, particularly if a small amount of silicone grease was placed under the copper thermocouple head. The iron-constantan thermocouple wires were made of thin wire for flexibility. The thermocouple head was held down by the weight of the ceramic support. The outside diameter of the ceramic support at its widest point was slightly less than one quarter inch in order to reduce contact with the cooling block

This contact caused the thermocouple to give temperatures slightly lower than the actual value. Since it was only necessary to confirm that the temperature of the glass slide each time a sample was sputtered was the same, and not necessary to know the exact temperature of the slide, this arrangement was satisfactory. Further refinements would be needed if the exact temperature were required.

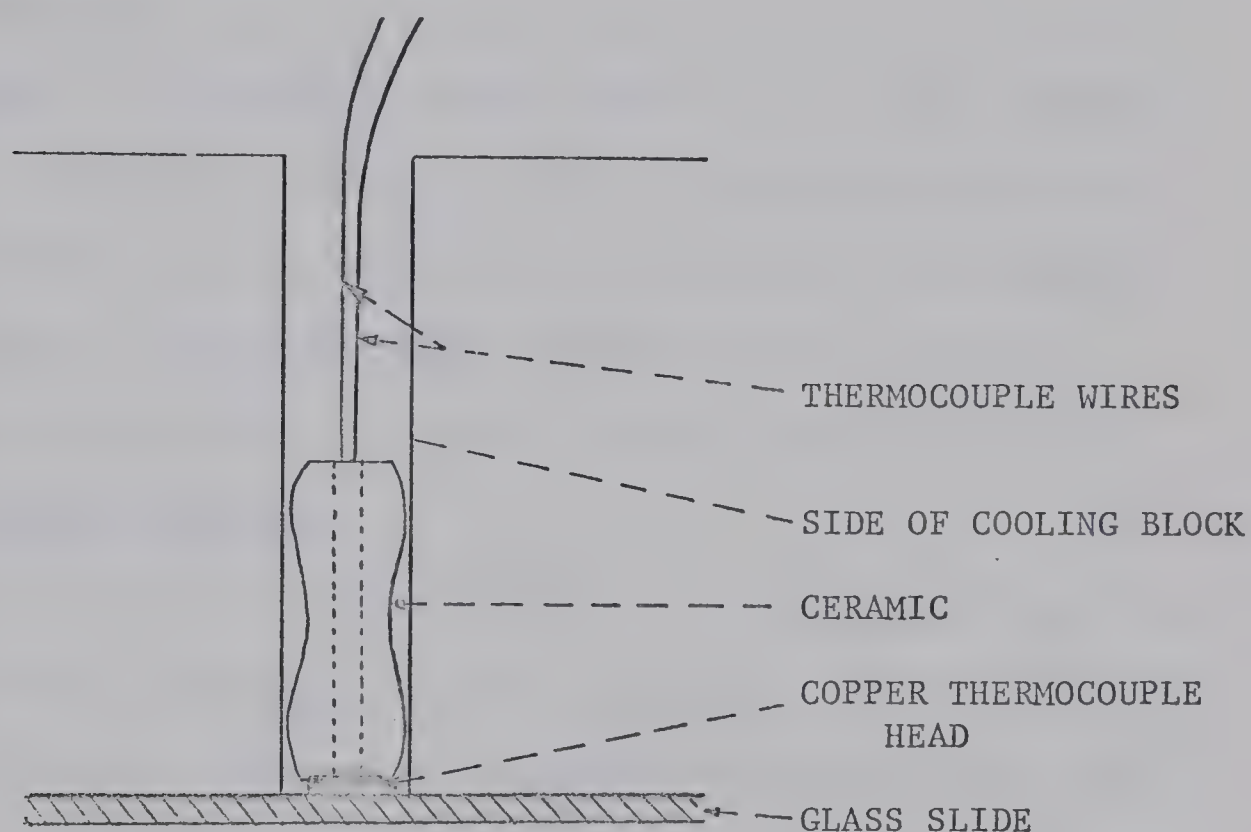


Figure 4.11 Cross Section of Thermocouple

4.9 Gas Mixing System

It was originally thought that it would prove advantageous to sputter in an oxygen and argon atmosphere since the argon would increase the sputtering rate. A gas mixing system was designed to permit mixing of two or more gases in any ratio of volumes in either of two ten litre storage tanks. These tanks were sufficiently large

enough that a controlled leak rate into the system at the maximum possible rate would decrease the pressure in the tanks by only five percent (5%) over one hour. Thus the leak rate and sputtering pressure would remain almost constant during the hour without constant adjustment. This system was tested but not used in making Hall effect samples as is described in section 5.6.

4.10 Air Admittance

Water vapor was originally removed from the air used to return the system to atmospheric pressure by passing the air through silica gel. Tests showed that the pump down time was not decreased compared to the time required using untreated atmospheric air. For this reason, silica gel was not used to remove water vapor from the air.

4.11 Film Thickness Monitor

A quartz crystal, film thickness monitor (Sloan Deposition Thickness Monitor DT-M3) was mounted on the top plate of the microcircuit jig above ports in the mask and slide holders. The thickness of the deposited film could be determined from the change in resonant frequency of the crystal. It was found that the monitor could not be used since very little of the sputtered material would diffuse up to the quartz crystal through the half inch port.

5. Preparation of Sputtered Silver Oxide Films

5.1 Introduction

From the preliminary studies described in Chapter 3, it was apparent that intrinsic films of silver oxide (Ag_2O) would have a resistance of 10^{11} ohms. As outlined in the next chapter, this resistance was much higher than could be used with any low noise, high input impedance semiconductor amplifier. It was thus necessary to produce low resistance films of silver oxide.

5.2 Determination of Slide Temperature

When Hall samples were sputtered in oxygen without cooling the slide, they were very thin, dark brown, and had a high resistance of 10^{10} ohms or greater. It appeared that at the high slide temperatures of about 100°C , the sputtered material would not coalesce to the glass slide.

When liquid nitrogen was used in the slide cooling system, samples sputtered in oxygen for an hour had an initial resistance in the range from 10^6 ohms to 10^7 ohms. Even though the bottom surface of the copper cooling block had been milled flat, and the block was clamped down on the glass slide, thermal contact between the cooling block and the glass slide was poor. The temperature of the glass slide was about -60°C to -40°C or far above the temperature of liquid nitrogen

(-196°C). When silicone grease was placed between the glass slide and the cooling block, the glass slide was maintained at a temperature of about -190°C during the sputtering. The films that formed at this temperature proved to be discontinuous. When cooled to liquid nitrogen temperatures, the silicone grease "blistered" and no longer maintained contact with all the glass slide. No deposit formed where the grease was still in contact with the slide. This problem was not encountered before by the other researchers who had sputtered silver oxide films at temperatures above that of liquid nitrogen. Suzuki² sputtered silver oxide at 5 torr air pressure without cooling. Rollins³ used a liquid nitrogen cooled anode but the substrate was probably at 0°C with a $380\text{ }\mu$ pressure. Lieberman and Medrud⁴ had substrates held in position with screws against a liquid nitrogen tank. Substrate temperatures of -50°C were probable with a sputtering pressure of $20\text{ }\mu$.

An $\text{Ag-Ag}_2\text{O-AgO}$ phase diagram (Figure 5.1) was constructed analogous to the $\text{Cu-Cu}_2\text{O-CuO}$ phase diagram⁵. The equilibrium line for $\text{Ag-Ag}_2\text{O}$ was obtained by Keyes and Hara⁶ using silver oxide crystals formed by the precipitation of silver nitrate and barium hydroxide. The melting point of Ag_2O is 815°C at 4625 atmospheres pressure⁷. The melting point of silver at one atmosphere is 960°C and the boiling point is 2212°C . The $\text{Ag}_2\text{O-AgO}$ line was based on the sputtering results.

The approximate sputtering region of the researchers has been marked in Figure 5.1. Suzuki sputtered at 0.3 torr without forming silver oxide, indicating that the substrate temperature was about $+50^{\circ}\text{C}$. Liquid nitrogen has a $10^5/T$ value of 1300 which is far to the right of diagram. Perhaps an unstable compound of silver oxide formed in that region and resulted in the poor deposit at liquid nitrogen temperatures.

s SUZUKI
r ROLLINS
l LIEBERMAN & MEDRUD
c CARNE

PRESSURE
 (ATMOSPHERES)

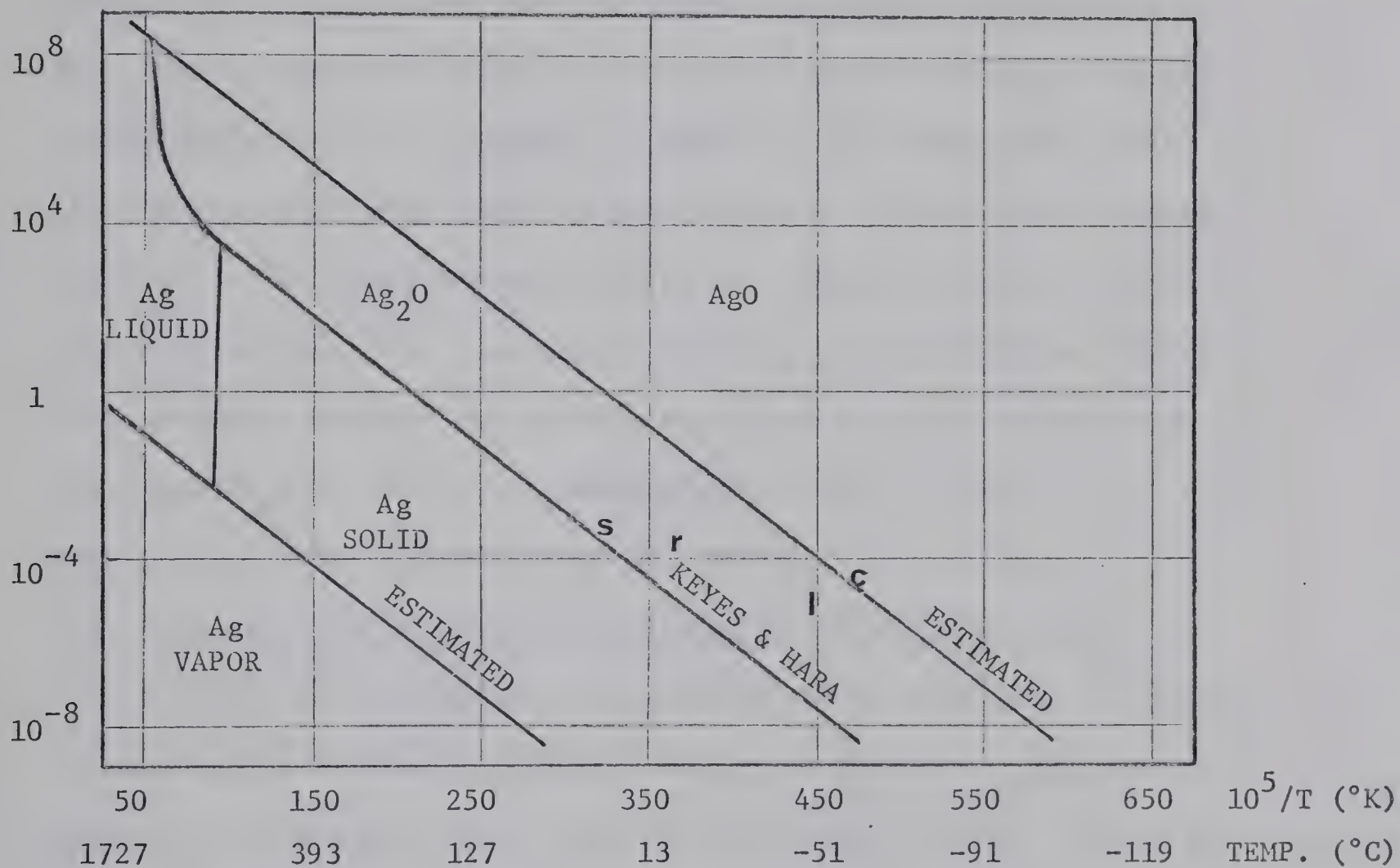


Figure 5.1 Ag-Ag₂O-AgO Phase Diagram

The slide temperatures of between -60°C and -40°C which were obtained when the cooling block rested on the glass slide were desired. The possibility of pumping alcohol cooled with dry ice (-55°C) through

the cooling system with silicone grease between the cooling block and the glass slide was considered. A constant slide temperature would be ensured. If the silicone grease were still to blister, some other material for thermal contact could be found. It was, however, very inconvenient to use the grease. The compression nuts between the cooling block and the copper tubing had to be undone each time a slide was sputtered in order to avoid contaminating the vacuum system with the grease. In addition, the compression nuts after repeatedly being loosened and tightened did not form a vacuum tight seal. To avoid the possibility of contaminating the diffusion pump with alcohol if a leak should develop, liquid nitrogen cooling with no grease between the cooling block and glass slide was used. Hall samples with an initial resistance between 10^6 ohms and 10^7 ohms were consistently produced using the method.

5.3 Determination of Optimum Sputtering Voltage and Pressure

A series of experiments were carried out to determine the effect of varying the sputtering voltage and oxygen pressure. Films were sputtered for one hour onto glass slides without a mask. Pressures of 15, 25 and 50 μ with voltages between 1000V and 2500V were chosen (Figure 5.2). The sputtering rate increased as the current increased.

This series of experiments showed that the film deposited across the 2" x 2" slide was more uniform at higher pressures when the greater diffusion of the silver and oxygen tended to even out any plasma inhomogenities. As pressures above 50 μ resulted in a glow discharge occurring

in the high voltage feedthrough line to the cathode, 40μ was chosen as a safe maximum pressure. The sputtering voltage was chosen to be 1500V with a current of 10 mA (15 watts). This gave a reasonable sputtering rate without overheating the sample.

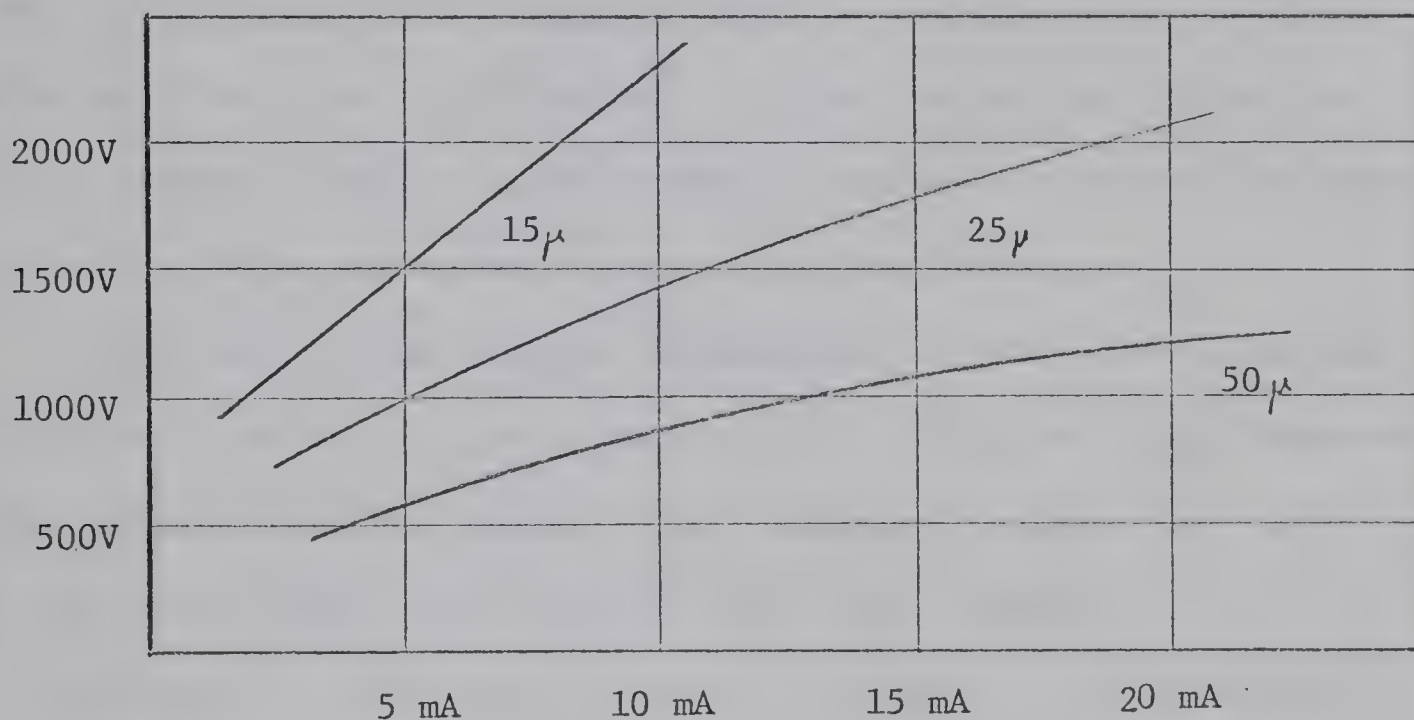


Figure 5.2 Relationships between Voltage, Current, and Pressure.

5.4 Preparation of Low Resistance (Ohmic) Electrical Contacts

The electrical contacts to the silver oxide samples were originally made of silver. The silver contacts were sputtered on the slide using the contact mask and an argon plasma (40μ , 2000V, 10 mA). The sample mask was then rotated into position below the slide and the silver oxide sample was sputtered in an oxygen plasma. Instead of the transition from silver to silver oxide resulting in an ohmic contact, a transparent yellow film formed at the silver contacts.

The apparent resistance of the films increased to greater than 10^{10} ohms even though the actual resistance of the silver oxide films was only 10^7 ohms. This yellow film was also formed if the silver oxide sample was sputtered first, followed by the silver contacts. Several researchers have suggested that the decomposition of silver oxide resulted from the formation of silver nuclei on the surface of the crystal. The end product should then be low resistance silver, and not the high resistance barrier which was formed.

Evaporated indium contacts adhered well to the glass slide but they also formed a high resistance contact. Evaporated gold contacts, which adhered well and formed a low resistance contact, were used on the samples upon which the Hall effect was measured.

Dynaloy 340 (conducting silver) was used to attach thin copper wire leads to the electrical contacts on the glass slide. The conducting silver formed a good mechanical bond to the glass slide over the temperature range from -150°C to 100°C .

5.5 Effect of Sputtering Time

The resistance of Hall samples sputtered for one half hour had a resistance of ten times the resistance of samples sputtered for one hour. Samples sputtered for two hours had a resistance of about half that of samples sputtered for one hour. The thin film effects on resistance were thus almost eliminated after sputtering for one hour.

Since continuous flow of liquid nitrogen through the cooling system required constant attention and was difficult to regulate, a sputtering time of one hour was chosen for the Hall samples.

5.6 Effect of Gas Composition

Several samples were prepared using a mixture of 75% oxygen and 25% argon. The resistance of the samples was about ten times those of samples sputtered in 100% oxygen. This was probably due to a greater sputtering rate for the silver combined with a slower rate of deposition for oxygen. In order to obtain low resistance films, the Hall effect samples were sputtered using pure oxygen.

5.7 Choice of Sample Position

Films sputtered without a mask showed that a quarter inch strip along the edge of the glass slide had a very thin deposit while the center $1\frac{1}{2}$ " x $1\frac{1}{2}$ " area appeared to be of uniform thickness. To check the uniformity of the center deposit, a mask was made to measure the resistance of 0.3 in. x 0.05 in. strips at six points along the glass slide. (Figure 5.3). Measurement of the resistance of several of these slides showed a general trend for the resistance to vary with position as in Figure 5.4. The cause for the variation of resistance could be due to slight differences in the slide temperature with position or to an inhomogenous plasma. Since there was no necessity to produce a large uniform sample, the situation was not remedied. A Hall sample mask was made with samples placed near the positions of the two minimum resistances. Samples made from this mask were used to measure

the Hall effect. The resistance of the high resistance sample was usually two to ten times larger than the other.

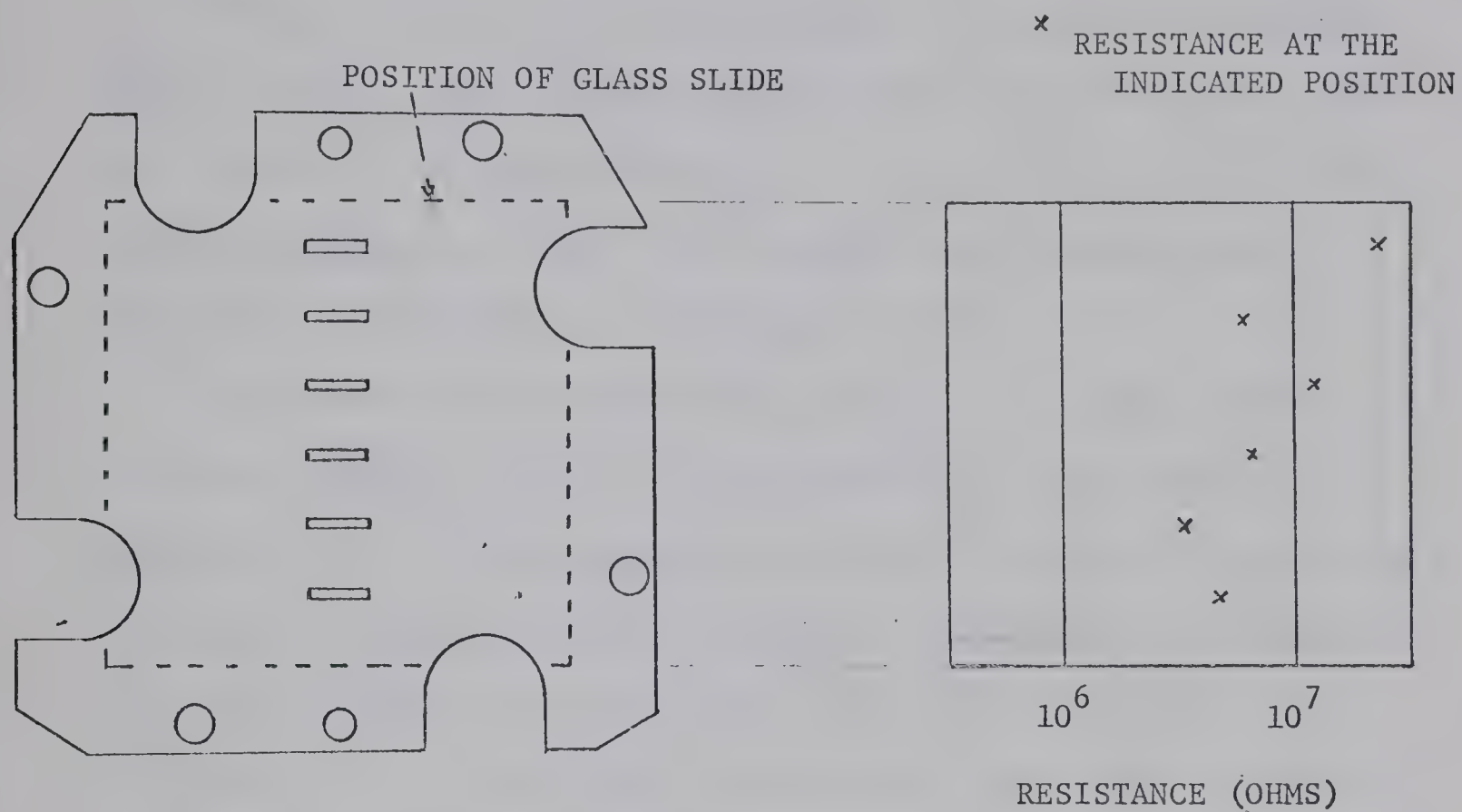


Figure 5.3 Mask for the
Determination of Resistance
versus Slide Position

Figure 5.4 Resistance versus
Slide Position

6. Design of Electrical Equipment

6.1 Methods of Measurement of the Hall Effect¹

The Hall voltage V_H is proportional to both the applied Hall sample voltage V_s and to the strength of the magnetic field B . The Hall voltage may be measured using either d.c. or a.c. for the sample voltage and magnetic field. The advantages and disadvantages of the various possibilities are discussed below.

Measurement of the Hall voltage using a d.c. sample voltage and a constant magnetic field is the best method for low resistance, stable materials. Strong homogeneous magnetic fields of 10,000 gauss are available from conventional magnets or 50,000 gauss from superconducting magnets. A potentiometer can be used on samples with a resistance of up to 10^5 ohms to balance out the offset voltage and measure the Hall voltage. Precise potentiometers and galvanometers are available which will permit measurement of voltages as low as 0.01 μ V on low resistance samples (e.g. 10 ohms). Samples with resistance above 10^5 ohms can be measured using a high impedance (10^{14} ohms) vibrating reed electrometer. The maximum resistance which a sample can have is limited by the capacitance of the circuit, sample holder, etc. When the time constant of the sample resistance and circuit capacitance becomes greater than one minute, measurement of even stable films is subject to errors due to drifting. The minimum detect-

able Hall voltage using a vibrating reed electrometer on a high resistance sample is about 1 to 10mV.

Measurement of the Hall voltage using an a.c. sample voltage and a constant magnetic field is the best method for high resistance samples with low carrier mobilities. By using feedback, a high input impedance amplifier may be built for amplifying small voltages that can not be measured by a d.c. amplifier. A band-pass filter is used to improve the signal to noise ratio. The use of an a.c. sample voltage also removes the d.c. voltage generated in a magnetic field if a temperature gradient exists in the sample(Nernst effect). The chief disadvantage of this method is that distortion in the applied sample voltage or in the balancing circuit limits the removal of the offset voltage. The minimum detectable Hall voltage is about 10 μ V to 100 μ V for stable samples in which the offset voltage does not drift.

Measurement of the Hall voltage using a d.c. sample voltage and a varying magnetic field is used only rarely. There is no advantage over using an a.c. sample voltage and a constant magnetic field. Additional disadvantages are the relative weakness of the magnetic field (5000 gauss) and the large magnitude of the electrical voltage induced by the varying magnetic field.

Measurement of the Hall voltage using a.c. for both the sample voltage and magnetic field provides an effective way to remove the

offset voltage. This can be seen by substituting into equation (2.14) values of $V_s = V_s \sin \omega_s t$ and $B = B \sin \omega_B t$. This gives :

$$V_H = \frac{\mu B V_s w 10^{-8}}{\ell} \sin \omega_s t \sin \omega_B t \quad (6-1)$$

$$= \frac{\mu B V_s w 10^{-8}}{2 \ell} [\cos (\omega_s + \omega_B) t - \cos (\omega_s - \omega_B) t] \quad (6-2)$$

The Hall voltage may be measured either at the sum frequency or at the difference frequency, but with the signal having only half the previous amplitude. By using a suitably designed bandpass filter, the offset voltage as well as the electric pickup voltage from the magnet are reduced to a value less than the Hall voltage. This is the best method to employ if the sample is unstable and the offset voltage drifts. One disadvantage of this method is that the strength of the varying magnetic field (5000 gauss) is smaller than that of the constant magnetic field so that the Hall voltage is smaller. Another disadvantage is that it is no longer easy to determine whether electrons or holes are the charge carriers of the silver oxide samples. It would be necessary to use a multiplier circuit and compare the phase of its output with that of the Hall voltage. The minimum detectable Hall voltage is limited by the noise voltage of the sample and the noise figure of the amplifier.

6.2 Selection of the Input Transistor for the Hall Voltage Amplifier

Selection of the best type of transistor for the input of the Hall Voltage Amplifier depended upon high input impedance plus the limitation described below.

An estimate of the magnitude of the Hall voltage was obtained by substituting typical values into equation (2-14). A mobility μ of $0.1 \text{ cm}^2/\text{volt-second}$ was chosen as being a reasonably low value. Using a magnetic field B of 10,000 gauss with a sample voltage of 10V and a l/w ratio of 4, the Hall voltage was calculated to be only 25 μ V. A larger voltage could have been obtained by increasing the sample voltage. A maximum value of 300V could have been used without appreciable heating of the sample. The difficulty in balancing out the increased offset voltage and the distortion associated with it would have limited the usefulness of increasing the sample voltage.

The minimum measurable Hall voltage depended upon the magnitude of the noise voltage in the sample. Part of this noise was associated with the decomposition of the silver oxide samples. The other part of the noise was due to random motion of electrons in the sample. The magnitude of this Johnson or thermal noise V_n is given by :

$$V_n = \sqrt{4 K T \Delta f R_s} \quad (6-3)$$

where K - Boltzmann's constant

T - temperature ($^{\circ}\text{K}$)

Δf - bandwidth of the amplifier (Hertz)

R_s - sample resistance (ohms)

The thermal noise voltage generated by various resistances for a bandwidth of one Hertz is given in TABLE 6.1

TABLE 6.1 Thermal Noise Voltage versus Resistance

R_s	V_n
10^6 ohms	$0.13\mu V$
10^7 ohms	$0.38\mu V$
10^8 ohms	$1.3 \mu V$
10^9 ohms	$3.8\mu V$
10^{10} ohms	$13 \mu V$
10^{11} ohms	$38 \mu V$

Noise is generated in an amplifier by circuit components such as transistors and resistors. The noise voltage at the output of an amplifier will thus be greater than the noise voltage in the sample times the gain A of the amplifier. The noise figure NF , used to indicate the relative amount of noise generated in the amplifier, is defined as :

(6-4)

$$N.F = 20 \log_{10} \frac{\text{Noise voltage at the output}}{A \times (\text{Thermal noise voltage from the sample resistance})}$$

From equations (6-3) and (6-4) it could be seen that in order to detect the Hall voltage in a sample with no decomposition noise and with a mobility of $0.1 \text{ cm}^2/\text{volt-second}$, the noise figure of the amplifier

with a one Hertz bandwidth must be less than 46 db for a sample with a resistance of 10^6 ohms and less than 26 db for a sample with a resistance of 10^8 ohms. Samples of intrinsic silver oxide could not be used as their noise voltage of $38\mu\text{V}$ for a bandwidth of one Hertz was larger than the expected Hall voltage.

Thus in addition to high input impedance, the amplifier required a low noise figure. Three types of transistors were considered for the input stage of this amplifier.

1) The ordinary junction transistor. An amplifier in the common emitter configuration can have an input resistance of 10^7 ohms. Complex feedback circuits⁸ have been reported with input impedances of 10^9 ohms. These circuits, however, possess a very high noise figure and thus could not be used (60 db).

2) The metal-oxide-semiconductor field effect transistor (MOS-FET). An amplifier in the common source configuration can have an input resistance as high as 10^{15} ohms d.c., or an input impedance of 10^9 ohms at low frequency a.c. signals due to input capacitance shorting. The MOS-FET at the time of the research, however, had a high noise figure of approximately 30 db. The noise figure for a MOS-FET amplifier would be at least 40 db. Because of this high noise figure, it would not be possible to measure samples with resistances greater than 10^6 ohms.

3) The junction field effect transistor (FET). An amplifier

in the common source configuration can have an input resistance of 10^{10} ohms d.c., or an input impedance of 10^9 ohms at low frequency a.c. signals due to input capacitance shorting. The noise figure is very low (0.5 db to 2.0 db) so that the noise figure for a FET amplifier would be about 5 db to 10 db. Using this type of amplifier, it is thus possible to measure samples with mobilities lower than $0.1 \text{ cm}^2/\text{volt-second}$ and resistances as high as 10^8 ohms. The junction FET was used to form the input to the Hall Voltage Amplifier which was used to measure the Hall effect of low resistance silver oxide films.

6.3 A.C. Voltage and Constant Magnetic Field

A circuit was constructed as shown schematically in Figure 6.1 for use with a 15 Hertz voltage and a constant magnetic field. The sample voltage supply provided two equal but opposite phase voltages across the sample so that the Hall contacts were near zero voltage. The outputs of two junction FET source amplifiers were put into the differential amplifier where any common mode signal was removed. The phase shift network and amplifier were used in an attempt to remove the offset voltage.

It was not possible to reduce the offset voltage to a level below the Hall voltage. A great deal of first harmonic (second order) distortion existed due to the dependence of the drain current on the square of the applied voltage. This is discussed in detail in section 6.4.3. A one volt distortion output voltage (30 Hertz) existed with

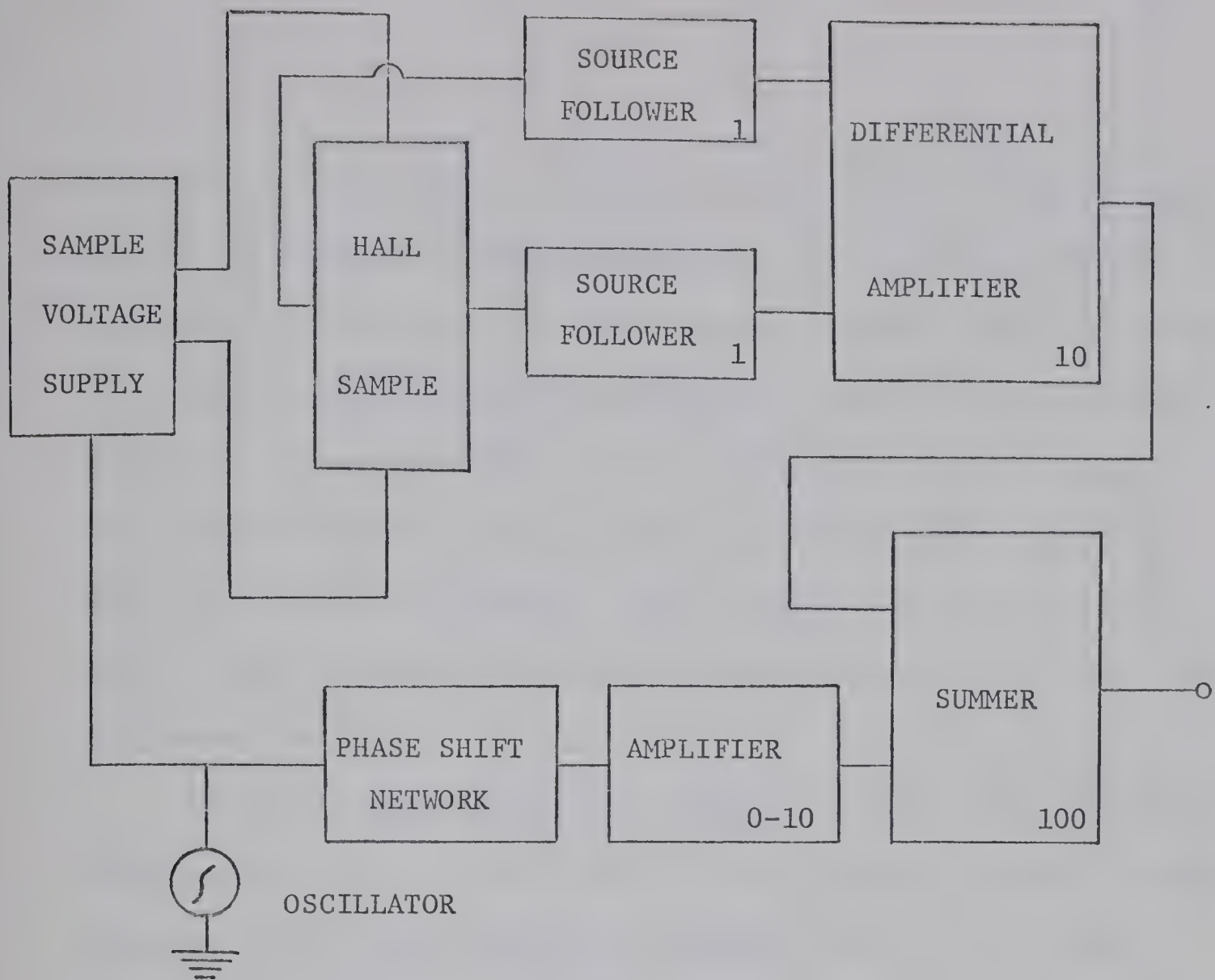


Figure 6.1 Schematic Diagram of the Circuit for Constant Magnetic Field

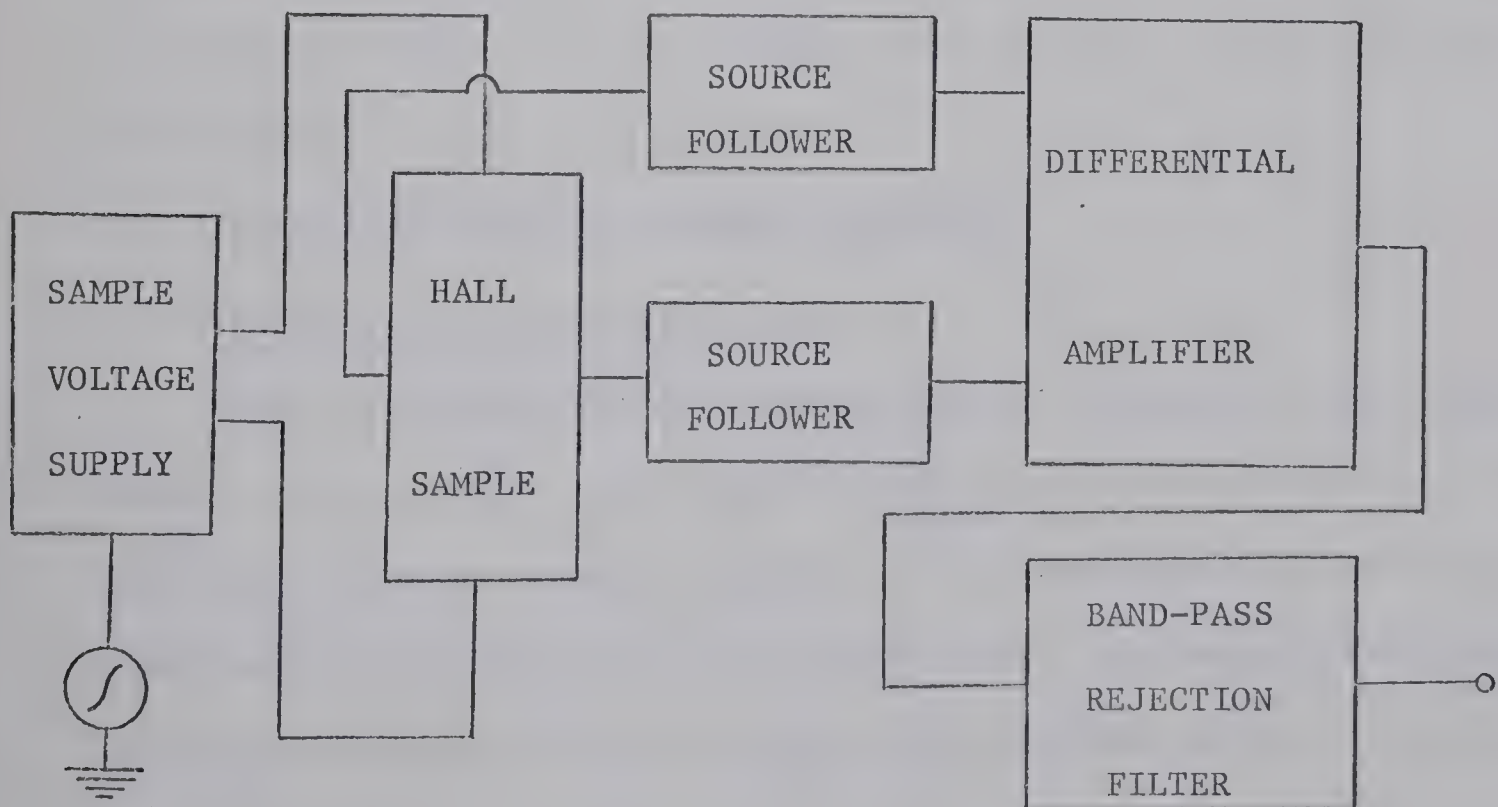


Figure 6.2 Schematic Diagram of the Circuit for Varying Magnetic Field

the offset voltage only two percent of the sample voltage of about 10 V. The smallest measurable mobility was $4 \text{ cm}^2/\text{volt-second}$. This could have been reduced by using a narrow bandpass filter or by increasing the gain of the source follower. The balancing circuit could not reduce the offset voltage below 200 mV at the output. This was equivalent to the voltage produced by a Hall sample of mobility $0.8 \text{ cm}^2/\text{volt-second}$. The balancing circuit adjustment was so sensitive that the phase shift and offset voltage could not be matched exactly.

Since the source follower - differential amplifier combination had a noise figure of only 5 db, it would be able to measure small voltages (1 μ V) when used with a bandpass filter. It was thus decided to measure the Hall effect using a.c. for both the sample voltage and the magnetic field. The schematic diagram of the circuit is shown in Figure 6.2. The design and performance of the circuit are discussed in the next section.

6.4 A.C. Voltage and Varying Magnetic Field

6.4.1 Construction of an A.C. Magnet

The a.c. magnet was constructed from a rectangular cored transformer. The original coils were removed and a slit was cut in one of the short sides as shown in Figure 6.3. An aluminum (i.e. non-magnetic) block was used to keep the cut portion apart. By using various sizes of shims, the width of the air gap could be varied in small increments

from zero to 0.3". Each of the two coils consisted of 275 turns of #16 magnet wire (0.05 inch diameter). The coils were connected in series.

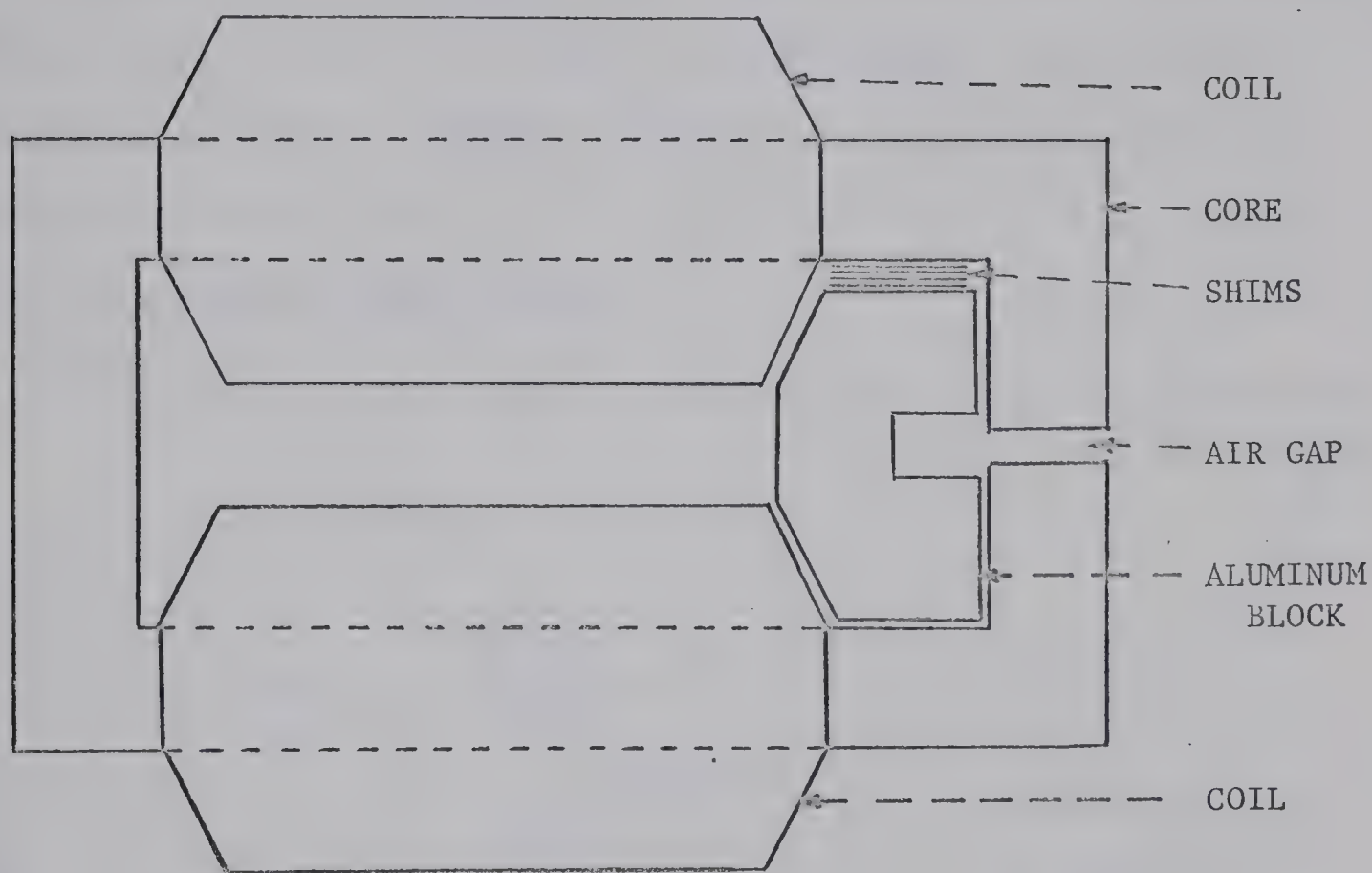


Figure 6.3 Cross-section of a.c. Magnet

The magnet was operated directly off the 115 volt mains which was a convenient source of power. It would otherwise have been necessary to design and build a stable, high powered oscillator to drive the magnet. The frequency was relatively constant at 60 ± 0.05 Hz. With an air gap of 0.1" the magnetic induction B as measured by a small Hall probe was found to be 4900 gauss and homogeneous to about five percent. At this setting, the coils remained cool during use.

There were two main problems in using the magnet. Vibration of the magnet caused the sample to move with respect to the magnetic field, inducing a small electric field into the Hall leads. Electrical grounding of the magnet itself was difficult since eddy currents induced about 100 mV in the core. It was possible with careful grounding of all the equipment to reduce voltage pickup in the Hall leads to less than 5 mV.

6.4.2 The Sample Voltage Supply

The sample voltage supply is shown schematically in Figure 6.4.

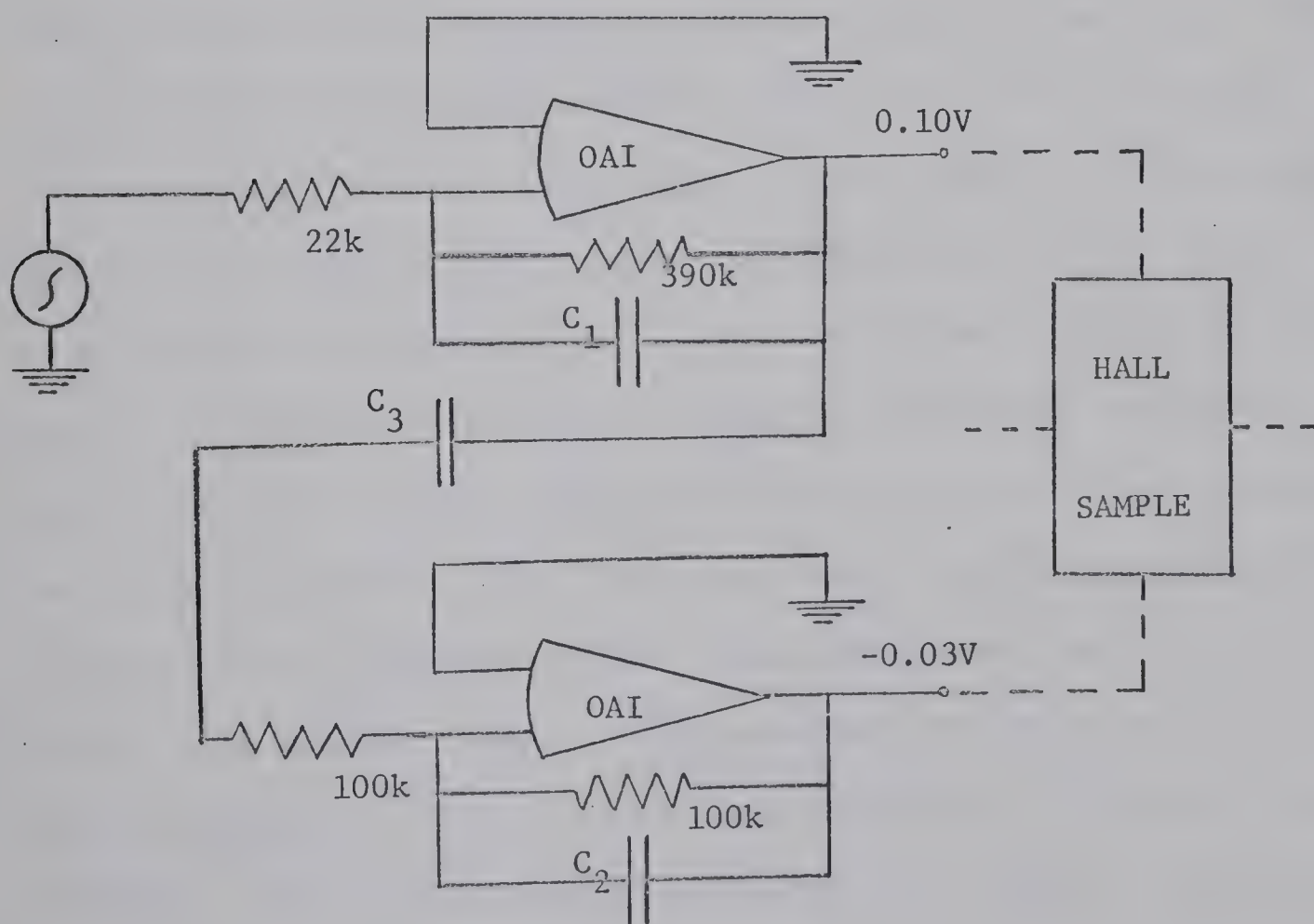


Figure 6.4 Schematic Diagram of the Sample Voltage Supply

A low frequency Hewlett-Packard (204B) oscillator was used to provide a sine wave at the desired frequency of 67 Hz. This battery operated oscillator was necessary as both the General Radio (Type 1305A) and the Hewlett-Packard (651) oscillators, which were powered from the 60 Hz. mains, produced a small voltage at the difference frequency. This 7 Hz. signal was about 3×10^{-5} the strength of the 67 Hz. main signal. Use of either of these two oscillators would have limited measurement of the Hall voltage to samples with mobilities μ greater than $5 \text{ cm}^2/\text{volt-second}$.

The first operational amplifier (OAI-Appendix III) in Figure 6.4 amplified the signal from the oscillator about eighteen times. The second operational amplifier inverted the polarity of the output voltage of the first with unity gain. The voltage across the sample was thus twice that of one operational amplifier. If the sample were uniform there would be no common mode signal as the Hall contacts were at the center of the sample. Due to inhomogeneities in the actual samples, a slight amount (2%) of common mode signal appeared at the Hall contacts. The common mode signal would have been reduced by varying the gain of the second operational amplifier if the common mode had been larger. The capacitors C_1 and C_2 limit the high frequency gain of the operational amplifiers and increase their stability. The capacitor C_3 maintains the d.c. output voltage near zero.

Experimentally it was found that the output of each operational amplifier could be 6.4 V (18 V peak to peak) without noticeable distortion.

6.4.3 The Hall Voltage Amplifier

6.4.3.1 The Source Follower Amplifier

The junction field effect transistor (FET) is comparable in performance to the pentode vacuum tube as shown in its characteristic curves in Figure 6.5 and Figure 6.6

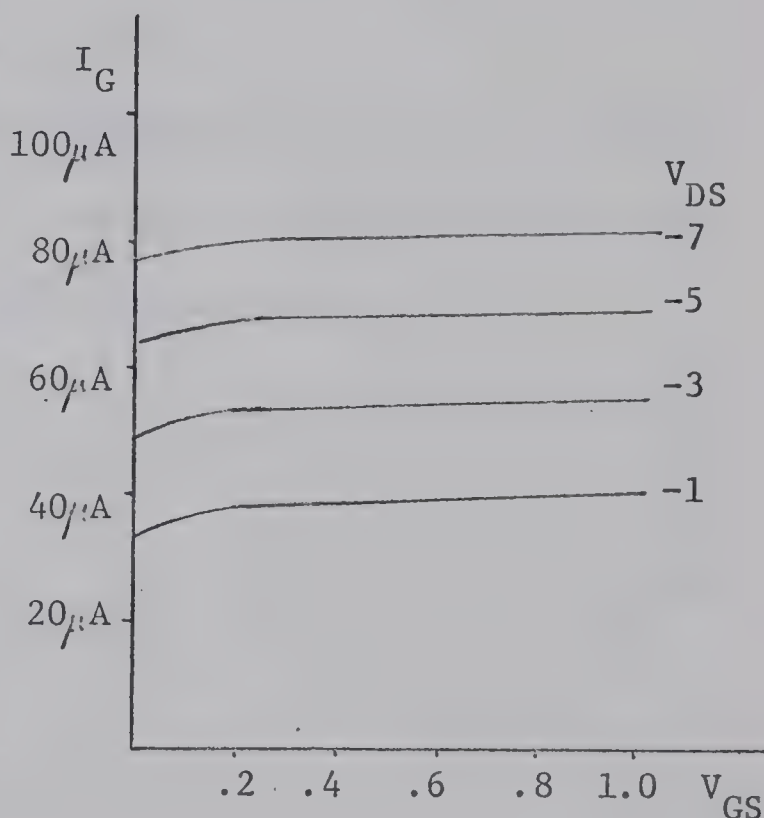
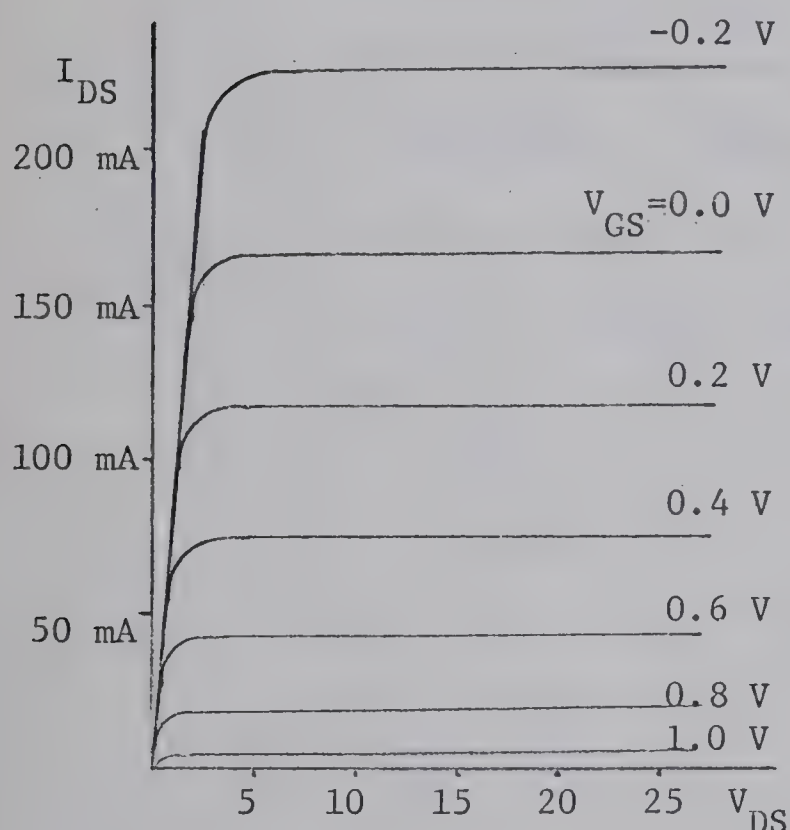


Figure 6.5 Drain Characteristics

Figure 6.6 Input Characteristics

When used as a source follower as shown in Figure 6.7, the input impedance is very high and the noise figure is low.

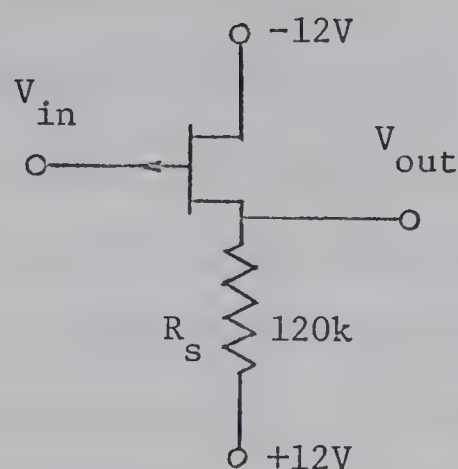


Figure 6.7 Basic Source Follower

The voltage gain A_V , input resistance R_{in} , output resistance R_{out} , and current gain h_{fs} can be expressed in terms of the common source y parameters using the following equations :

$$A_V = \frac{y_{fs} R_s}{1 + y_{fs} R_s} \quad (6-5)$$

$$R_{in} = 1 / y_{is} \quad (6-6)$$

$$R_{out} = R_s // 1/y_{fs} \quad (6-7)$$

$$h_{fs} = y_{fs} / y_{is} \quad (6-8)$$

Typical y values for the 2N2842 (Siliconix) transistor which was used with a drain current I_D of 50 μ A are :

$$y_{is} : 20 \times 10^{-12} \text{ mhos}$$

$$y_{rs} : 6 \times 10^{-12} \text{ mhos}$$

$$y_{fs} : 250 \times 10^{-6} \text{ mhos}$$

$$y_{os} : 0.42 \times 10^{-6} \text{ mhos}$$

The voltage gain of the basic source follower is thus calculated to be 0.78, the input resistance is 5×10^{10} ohms, the output resistance is 3900 ohms, and the current gain is 1.25×10^7 .

A biasing circuit for the d.c. gate current is required to stabilize the source follower when the input is open circuit and to prevent the gate current from flowing through the high resistance sample. Distortion is reduced if the voltage gain is increased by increasing the effective value of the current gain. This is best done by adding a high beta npn junction transistor in complementary compound configuration. These are shown in Figure 6.8.

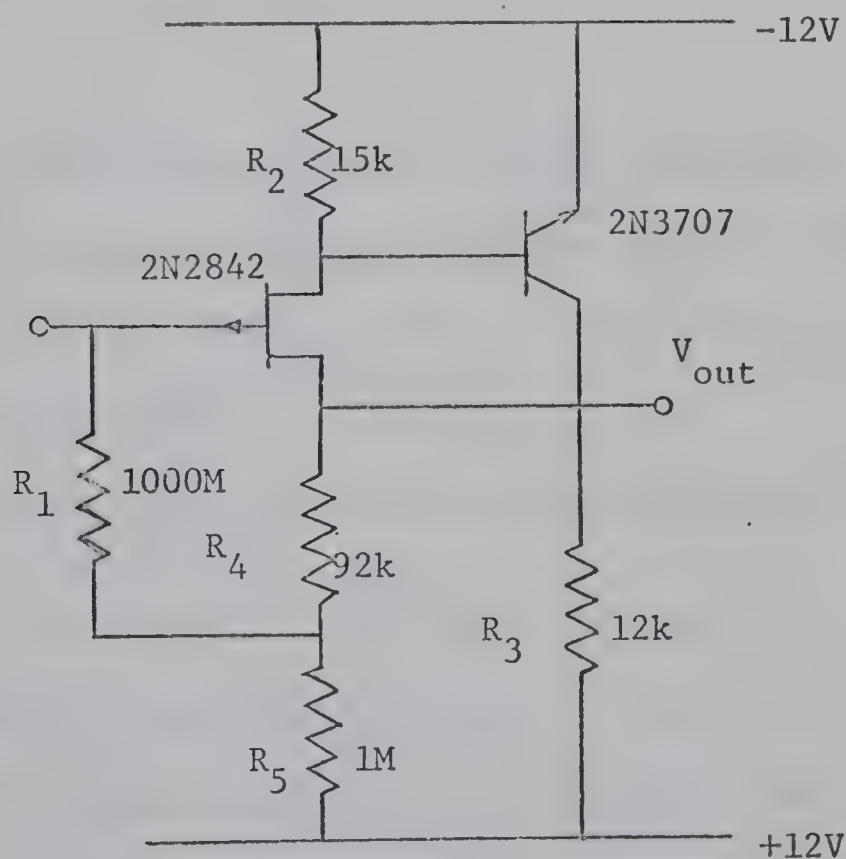


Figure 6.8 Complementary Compound FET Source Follower

The following relationships now hold.

$$A_v' = \frac{y_{fs} h_{fe}' [R_3 // (R_4 + R_5)]}{1 + y_{fs} h_{fe}' [R_3 // (R_4 + R_5)]} \quad (6-9)$$

$$R_{in}' = R_1 \left(1 - \frac{A_v' R_5}{R_4 + R_5} \right) // \frac{1}{y_{is}} \quad (6-10)$$

$$R_{out}' = \frac{1}{y_{fs} h_{fe}'} // \frac{1}{R_3 // (R_4 + R_5)} \quad (6-11)$$

$$h_{fs}' = y_{fs} h_{fe}' / y_{is} \quad (6-12)$$

where the current gain h_{fe}' of the npn transistor is reduced from 350 to 200. Using the component values shown in Figure 6.8, it is found that A_v' is 0.998, R_{in}' is 1.2×10^{10} ohms, R_{out}' is 20 ohms, and h_{fs}' is 2.5×10^9 .

The input capacitance of the FET is given by :

$$C_{in} = C_{GD} + C_{GS} (1 - A_v') \quad (6-13)$$

For the 2N2842 transistor, $C_{GD} = C_{GS} = 7$ pf. At a frequency of 67 Hz., this gives an input reactance of 3.4×10^8 ohms. This is a low value but it was necessary since the frequency of the magnet was fixed

at 60 Hz. It would have been possible to have used a sample voltage frequency of 54 Hz., but this would have only increased the reactance to 4.2×10^8 ohms. The sample voltage frequency was chosen at the higher value of 67 Hz. in order to obtain the larger difference in gain between the sample voltage frequency and the difference frequency.

The amplifier shown in Figure 6.8 was used in an attempt to measure the Hall voltage with a constant magnetic field as is described in section 6.3. When used with a varying magnetic field, it was found that a 7 Hz. voltage was produced at the output of the whole circuit even though the Hall sample was not placed between the poles of the magnet. This was due to the dependance of the drain current on the square of the gate to source voltage as given by equation (6-14). Thus mixing occurred between the 67 Hz. sample voltage and 60 Hz. pickup voltage, producing the 7 Hz. signal,

$$I_D = I_{DSS} \left(\frac{V_{GS}}{V_p} - 1 \right)^2 + I_{GSS} \quad (6-14)$$

where I_D - drain current

I_{DSS} - drain current at zero gate voltage

V_{GS} - gate to source voltage

V_p - gate to source pinch-off voltage

I_{GSS} - gate to source cut-off current

Since

$$V_{GS} = V_{GSQ} + (1-A) V_{67} \sin \omega_{67} t + (1-A) V_{60} \sin \omega_{60} t \quad (6-15)$$

it can be shown that

$$I_D = 2 I_{DSS} \frac{(1-A)^2 V_{60} V_{67}}{V_p^2} \sin \omega_{60} t \sin \omega_{67} t + \text{other terms} \quad (6-16)$$

From equation (6-16) it can be seen that the strength of the 7 Hz. distortion can be reduced by making the gain closer to unity. This was achieved by replacing the source resistance R_3 with a transistor current source as shown in Figure 6.9. The transistor was chosen to have a low h_{ob} (1.2×10^{-7} mho for the 2N4058).

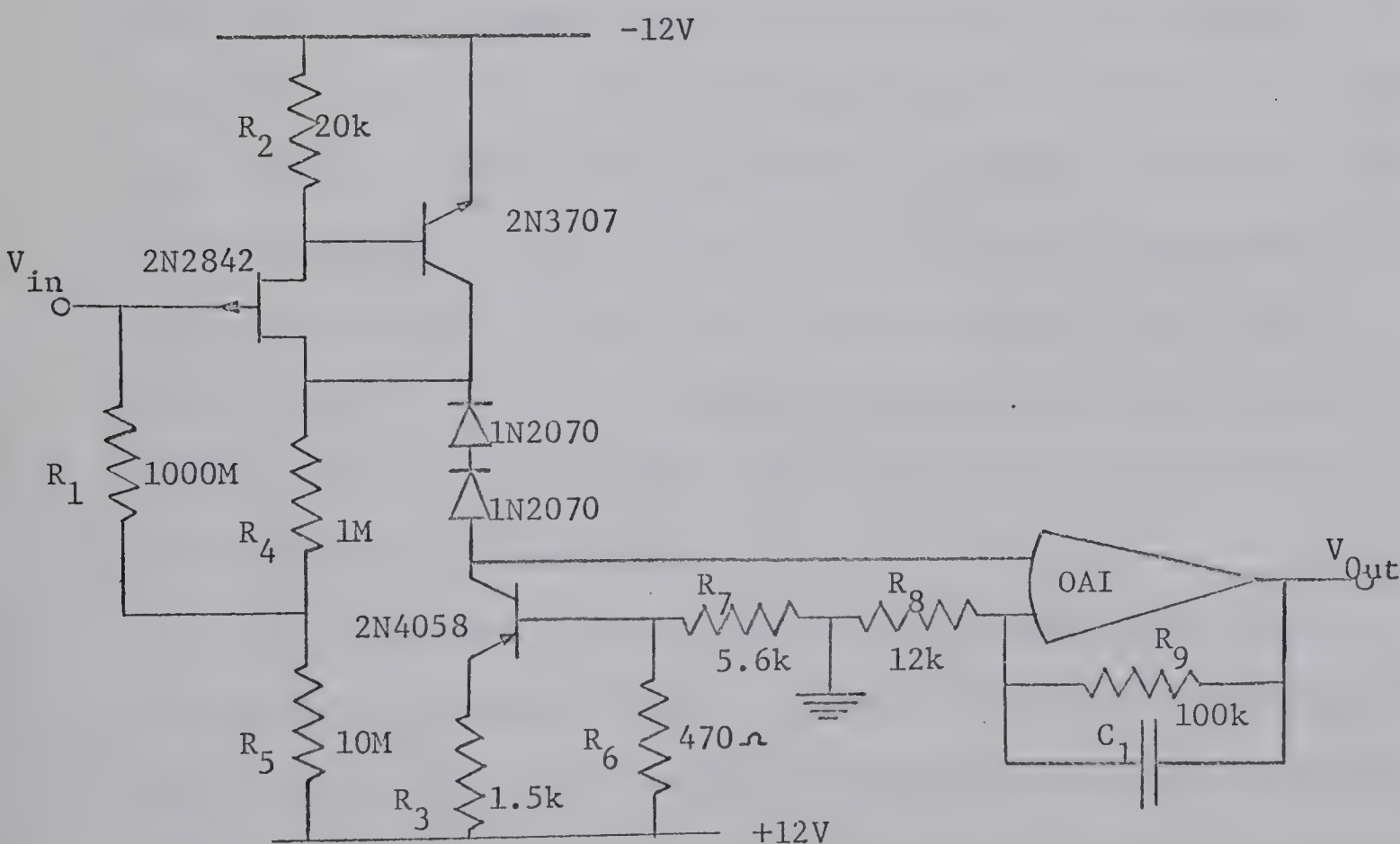


Figure 6.9 Source Follower with Current Source

The effective source resistance consists of $1/h_{ob}$, the gate leakage current biasing network, and the input impedance of the amplifier at the output of the source follower in parallel. The gate leakage current resistor values were increased about ten times to 11×10^6 ohms. To supply the high input impedance the output was taken through an OAI operational amplifier with a gain of nine and an input impedance of 10^7 ohms.

The two 1N2070 diodes were used to adjust the d.c. level to the input of the operational amplifier to near zero volts.

6.4.3.2 The Differential Amplifier

The differential amplifier and two source followers which were described in the previous section form the Hall Voltage Amplifier as shown in Figure 6.10. The differential amplifier removed the common mode voltage. The Hall Voltage Amplifier amplified the offset and the Hall voltages eighteen times. If the offset voltage were 2% of the sample voltage of 12 V the output voltage would be twelve volts peak to peak, or near the distortion level. A gain much higher than eighteen was thus not possible although it would have reduced the noise figure of the amplifier.

The capacitors C_1 and C_2 were used to prevent the output of the differential amplifier (OAI-Appendix III) from being affected by d.c. voltage levels at the output of the source follower amplifiers. The capacitor C_3 was necessary to limit the high frequency response of the differential amplifier in order to prevent oscillation.

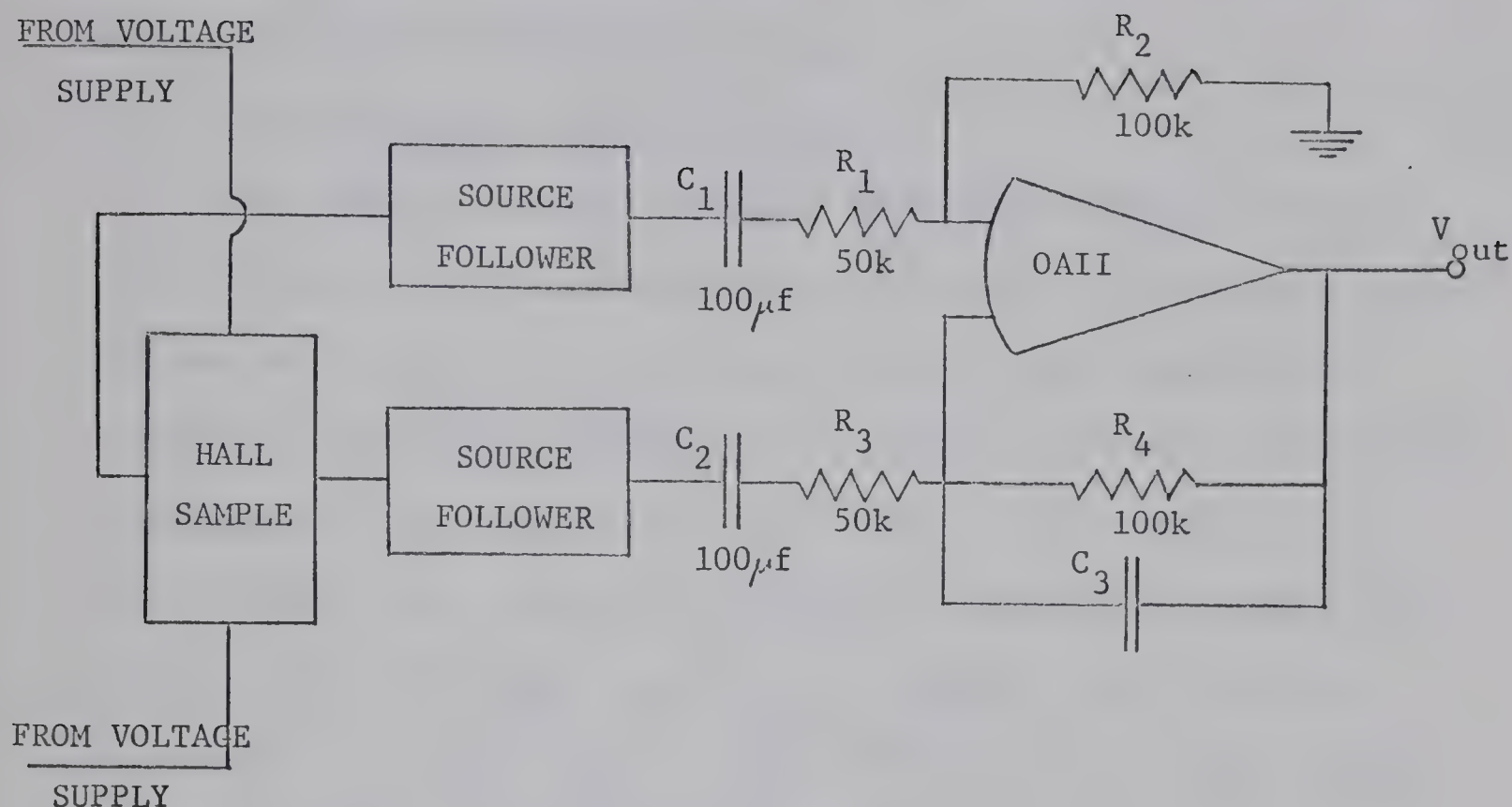


Figure 6.10 Hall Voltage Amplifier

The differential amplifier had a gain A of two. Since the gain of the positive input terminal is $(A + 1) / A$, the voltage divider R_1 and R_2 reduced the gain such that :

$$R_2 (A + 1) / A (R_1 + R_2) = 1 \quad (6-17)$$

The components of the differential amplifier were carefully selected to obtain the maximum common mode rejection ratio (C.M.R.R.). Capacitor C_3 was chosen as small as possible. The inputs of the two source followers were joined together and a 67 Hertz voltage applied

to them. Resistors R_1 and R_2 were selected so as to minimize the output of the differential amplifier. By this method a common mode rejection ratio of 40,000 was obtained.

6.4.4 The Band-Pass - Rejection Filter

The output of the Hall Voltage Amplifier contained the 7 Hz. Hall voltage as well as other undesired voltages. The thermal noise voltage at the input was expected to be 1 μ V for a bandwidth of one Hertz. The offset voltage (67 Hz.) and pickup voltage (60 Hz.) at the input was expected to be 0.2 V or less. Thus a difference in gain between 7 Hz. and 60 Hz. of 110 db or larger was required. The gain of the Hall Voltage Amplifier was eighteen. The band-pass - rejection filter had a gain of about 1000 so that the output could easily be observed with an oscilloscope.

A schematic of the band-pass - rejection filter is shown in Figure 6.11. It consisted of a 7 Hertz band pass filter, a 67 Hertz twin - T rejection filter, an OAI amplifier, a 60 Hertz twin - T rejection filter and an OAI amplifier. The operational amplifiers were necessary not only to supply gain but also to provide a high output impedance and low input impedance for the filters in order to obtain as high a rejection as possible

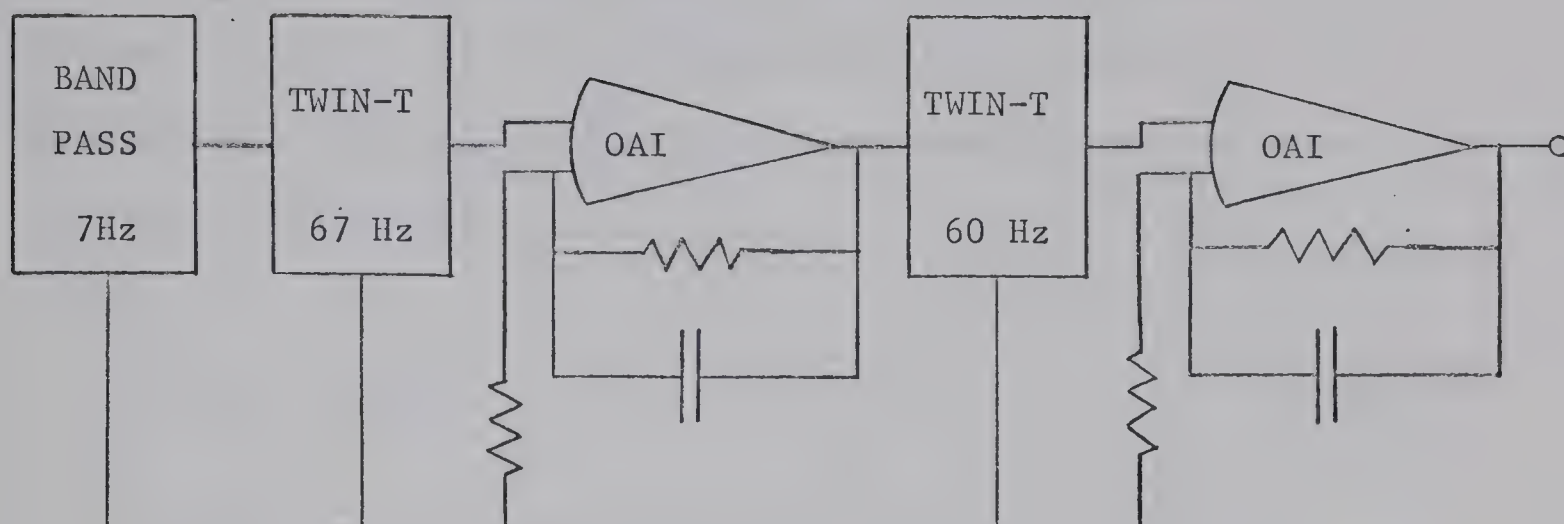


Figure 6.11 Band-Pass - Rejection Filter

The Band-Pass Filter is shown in Figure 6.12.

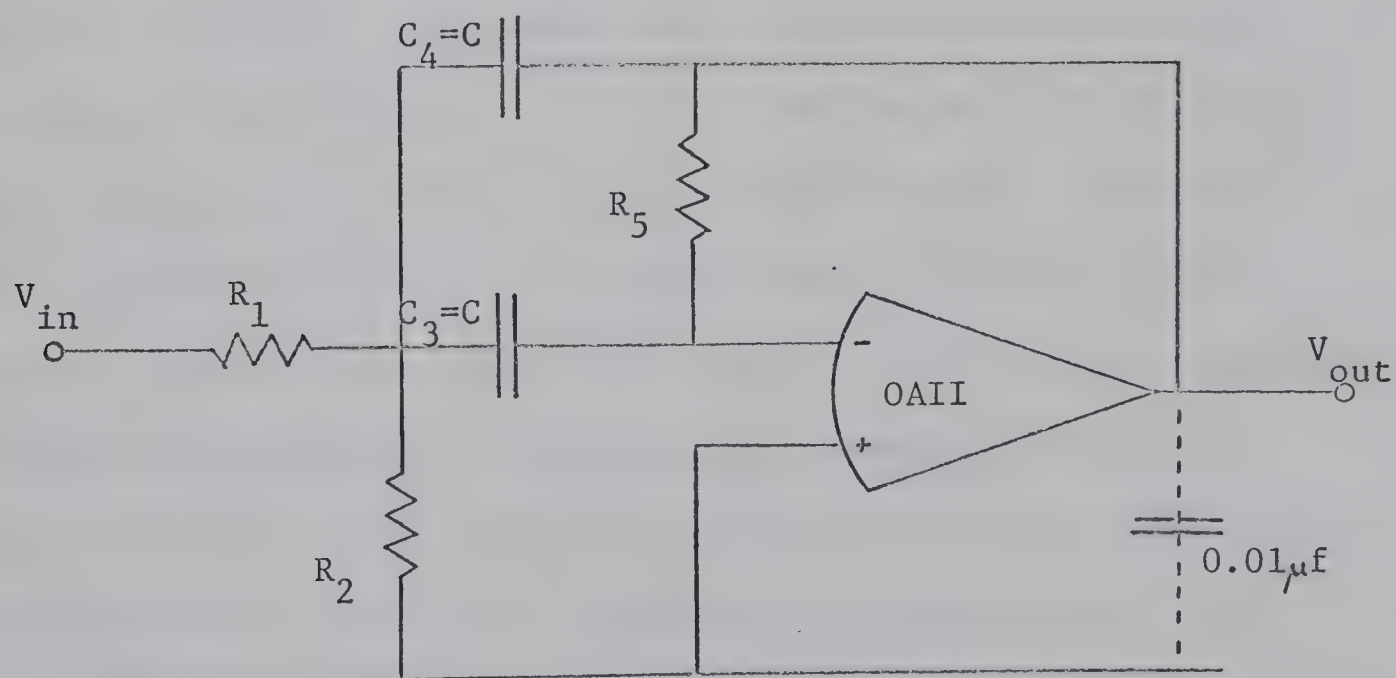


Figure 6.12 Band-Pass Filter

The gain A was chosen to be 10 with a center frequency f_c of 7 Hz and a Q factor of 10. Two capacitors were obtained with a capacitance $C = C_3 = C_4 = 1.064 \mu\text{f}$. The resistance values were calculated as follows :

$$K = C \times 2 \pi f_c \quad (6-18)$$

$$R_1 = \frac{Q}{A K} = 21.36 \times 10^3 \text{ ohms} \quad (6-19)$$

$$R_2 = \frac{Q}{(2Q^2 - A)} \quad K = 1.124 \times 10^3 \text{ ohms} \quad (6-20)$$

$$R_5 = \frac{2Q}{K} = 427.2 \times 10^3 \text{ ohms} \quad (6-21)$$

The Q factor of ten (10) was chosen to give a bandwidth of approximately one Hertz. A narrower band filter could be built to provide a lower noise voltage, but if the line frequency (60 Hz.) were to change, the gain would then be reduced significantly. The OAI operational amplifier was used as the OAI operational amplifier did not produce a filter of the calculated response. The 0.01 μf capacitor at the output was necessary to prevent high frequency oscillation.

Figure 6.13 shows the frequency response of the band-pass filter. The gain of the 60 Hz. and 67 Hz. frequencies is approximately 0.1.

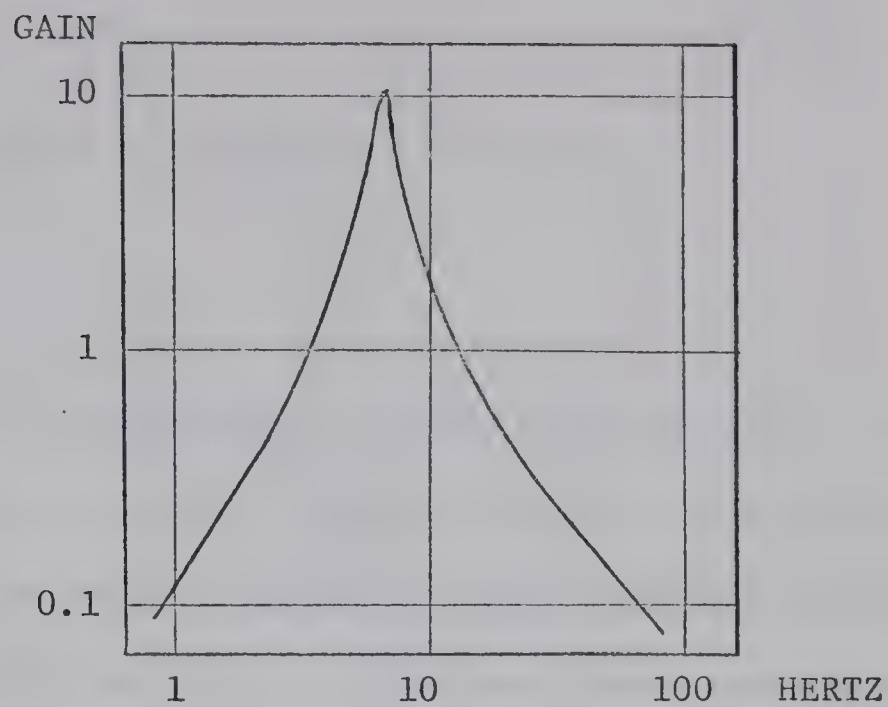


Figure 6.13 Frequency Response of the Band-Pass Filter

The general form of the twin - T rejection filter and OAI amplifier is shown in Figure 6.14.

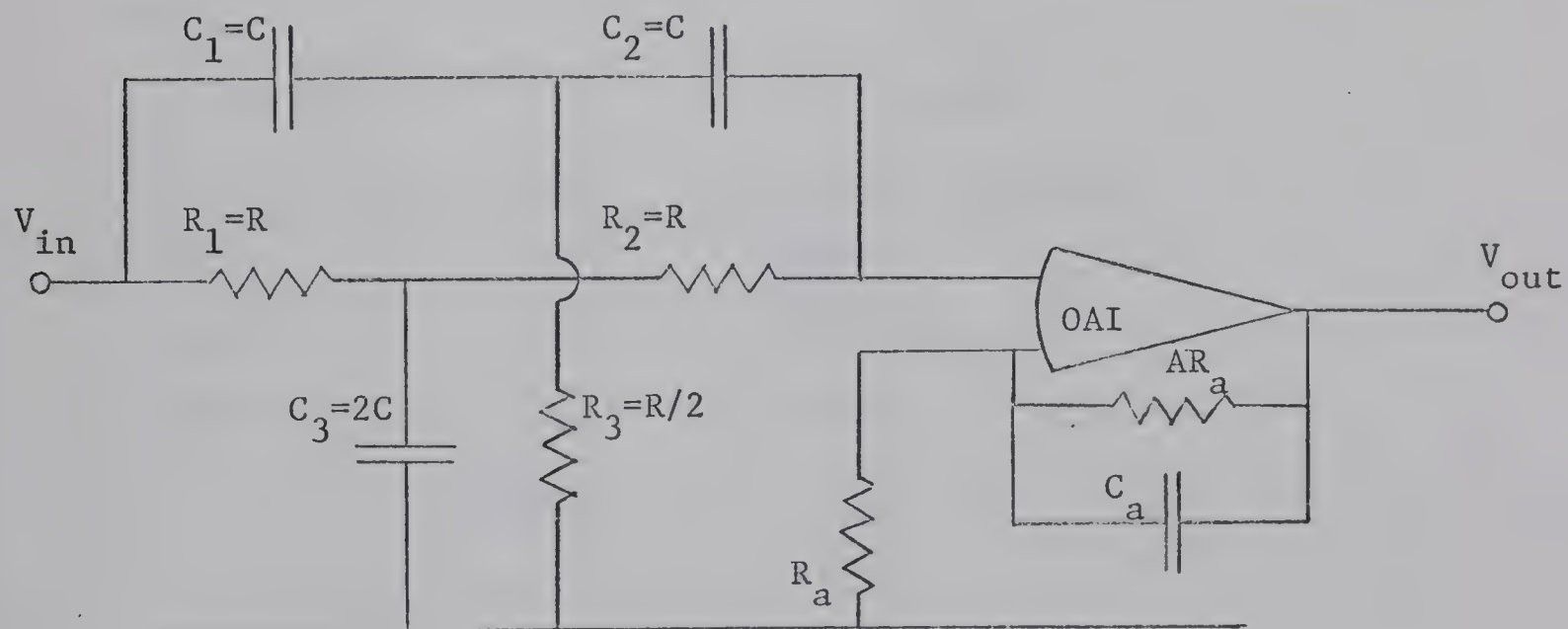


Figure 6.14 Twin - T Rejection Filter and Amplifier

The rejection frequency f_r is given by

$$f_r = 1/2 \pi R C \quad (6-22)$$

Infinite rejection is theoretically possible if exact values of components are used. Component values were thus carefully chosen so as to maximize the rejection. Further high frequency rejection was possible by means of C_4 which was chosen large enough to supply a frequency cut-off of 30 Hz. This capacitor also helped to remove the 120 Hz. and 127 Hz. sum frequencies. The d.c. gain of the operational amplifier was about 12.5 with an a.c. gain at 7 Hz. of 10.

The values chosen for the 60 Hz. and 67 Hz. twin - T filters were

60 Hertz.		67 Hertz.
0.492 μ f, 0.492 μ f	C_1	0.483 μ f, 0.485 μ f
0.988 μ f	C_2	0.968 μ f
5.38 K Ω	R_1	4.918 K Ω
2.69 K Ω	R_2	2.46 K Ω

$$R_a = 12 \text{ K}\Omega$$

$$AR_a = 150 \text{ K}\Omega$$

$$C_a = 0.33 \text{ } \mu\text{f}$$

$$A = 12.5$$

The frequency response of the combined Band-Pass - Rejection Filter is shown in Figure 6.15. There is 120 db difference in gain between the 7 Hz. and 60 Hz. frequencies. Band-width of the filter is 0.7 Hertz.

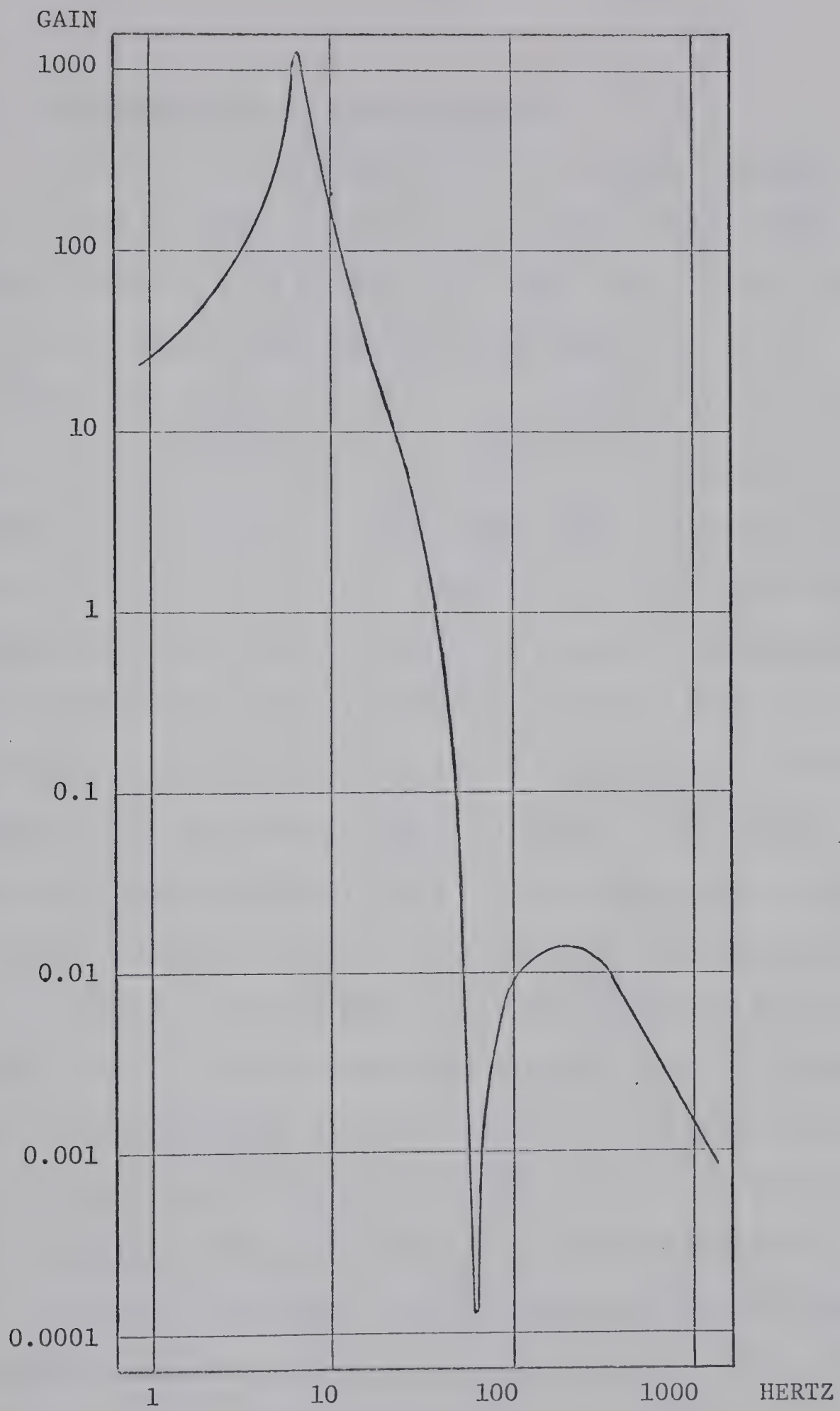


Figure 6.15 Frequency Response of the Band-Pass-Rejection Filter

6.4.5 Performance of the Complete Circuit

The gain of the complete circuit was 21,000. The noise level was less than 1 μ V when referred to the input. Noise figure of the complete circuit was 13 db with a 10^6 ohm resistor at the input and 7 db with an 8×10^6 ohm resistor at the input.

The input impedance of the source followers at 67 Hz. was measured to be 2×10^8 ohms for one and 5×10^8 ohms for the other, indicating a difference of input capacitance of the two FET's. The gain of the source followers as measured by a dual input oscilloscope increased from 0.996 to 0.9997 when the transistor current source replaced the source resistor. When 0.5 V of both 60 Hz. and 67 Hz. was applied at the input of both source followers, there was no increase in the magnitude of the 7 Hz. signal at the output of the band-pass - rejection filter. A 1 mV 7 Hz. signal was produced by each of the source followers, but this was removed by the differential amplifier.

An indium antimonide Hall sample was calibrated in a known d.c. magnetic field. When the sample was placed in the a.c. magnetic field, a Hall voltage of 1.9 V was measured. The peak magnitude of the field was then calculated to be 4920 gauss. This agreed favorably with the value of 4900 gauss measured by a R.F.L. Gaussmeter.

Because the magnitude of Hall voltage was close the noise level, a test was made to determine the minimal detectable Hall voltage. The current through the indium antimonide was reduced until the Hall

voltage was just detectable at this point, the Hall voltage had a value of half of the noise voltage. The Hall voltage could be easily measured if it were twice the noise voltage or greater. For example, if the Hall sample generated only Johnson thermal noise, a voltage as low as $0.4 \mu\text{V}$ could be detected for a 10^7 ohm sample. The minimum mobility of a sample which could be detected was thus $2.7 \times 10^{-3} \text{ cm}^2/\text{volt-second}$. Decomposition noise in the silver oxide samples however, raised the minimal detectable voltage.

7. Results

7.1 Properties of Silver Oxide Films

The silver oxide samples were originally dark brown and opaque. The films would become transparent after a period of two to three weeks.

The resistance of the samples was measured as soon as air could be admitted to the system - about thirty minutes after sputtering had stopped. The resistance of the samples was then about 10^6 ohms to 10^7 ohms. In most samples this resistance would decrease to one half to one tenth of the initial value, perhaps due to the silver oxide film annealing. The resistance would then slowly increase, with the rate of increase of resistance dependent on the individual samples. Usually the high resistance samples increased in resistance quickest. The highest resistance reached was about 10^{11} ohms. Thereafter the samples would decompose to a resistance of about 10^5 ohms. The change in resistance with time is shown in Figure 7.1 for an average sample.

The resistance of several samples was measured at elevated temperatures. The samples were found to decompose at temperatures above 100°C . This is much lower than the temperature values obtained by Keyes and Hara⁶ using precipitated samples of silver oxide (Ag_2O).

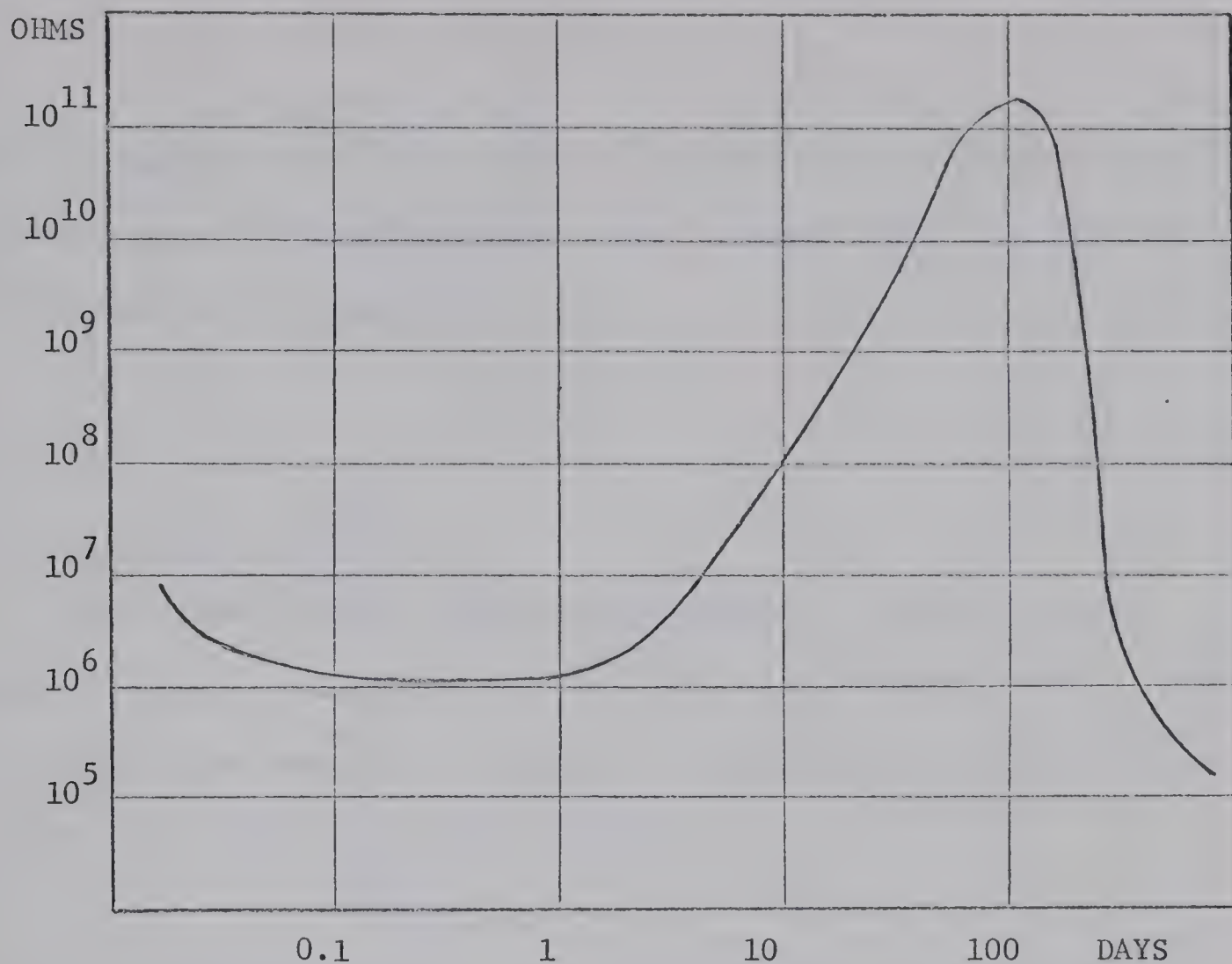


Figure 7.1 Variation of Resistance with Time

Usually the resistance of the sample would double after first being heated to 80°C and returned to room temperature. The samples could then be heated and returned to room temperature with the same resistance that they had before being heated.

Assuming that the resistance R varies as :

$$R = R_o T^{-3/2} \exp (E/2 K T) \quad (7.1)$$

where R_o - constant

E - band gap energy

K - Boltzmann's constant

T - temperature (°K)

$T^{-3/2}$ - assumed temperature variation of mobility

the band gap was found to be 0.31 eV for samples with a resistance of 10^6 ohms to 10^7 ohms and 0.57 eV for a sample with a resistance of 10^8 ohms at room temperature.

7.2 Hall Effect Measurement

Four silver oxide samples were measured. Only one sample produced a Hall voltage greater than the noise voltage. The Hall voltage was measured on this sample with time at room temperature. The results are shown in TABLE 7.2.

TABLE 7.2

<u>Days</u>	<u>Noise Voltage</u>	<u>Hall Voltage</u>	<u>Mobility</u>
0.5	1 μ V	1.5 μ V	0.020 $\text{cm}^2/\text{volt sec.}$
1.5	1.7 μ V	3.4 μ V	0.046 $\text{cm}^2/\text{volt sec.}$
5	2.1 μ V	4.2 μ V	0.056 $\text{cm}^2/\text{volt sec.}$
6	2.5 μ V	5.0 μ V	0.067 $\text{cm}^2/\text{volt sec.}$
8	-	5.0 μ V	0.067 $\text{cm}^2/\text{volt sec.}$
10	2.9 μ V	3.4 μ V	0.046 $\text{cm}^2/\text{volt sec.}$
12	2.9 μ V	-	-
14	3.4 μ V	-	-

The noise voltage increased steadily with time. The Hall contact resistance 12 hours after sputtering was 2.5×10^6 ohms. The Johnson thermal noise of the sample would be 0.2 μ V, but the noise figure of the amplifier would raise this to 0.9 μ V times the gain of

the amplifier at the output. The measured value of $1.0 \mu\text{V}$ indicated only Johnson noise was present in the sample. A day later, the sample resistance was approximately the same but the noise voltage had risen to $1.7 \mu\text{V}$. It thus appeared that the sample was stable the first day, possibly in the Ag_2O form of silver oxide. The sample then started to decompose, which resulted in the additional noise voltage of the sample.

The mobility increased for the first six days, and then started to decrease. The silver oxide film was apparently slowly annealing into a more crystalline form. This resulted in easier passage of the charge carriers through the sample and an increase in the mobility. After eight days the decomposition had proceeded to such an extent that the carrier mobility started to decrease. The Hall voltage then became less than the noise voltage.

8. Conclusions

It was possible to observe the Hall effect of high resistance materials with a mobility less than $0.01 \text{ cm}^2/\text{volt-second}$ using the electronic circuits designed for measurement with a.c. electric and magnetic fields. The value of $0.01 \text{ cm}^2/\text{volt-second}$ is the normal lower limit to the mobility measurement. The low noise amplifier constructed was limited in measurement of the Hall voltage by the noise voltage of the sample and the amplifier.

A number of improvements can be made :

1) A multiplying circuit may be constructed so that the phase of the Hall voltage can be obtained. This will directly determine whether the conduction is n or p type.

2) The sample voltage may be increased in order to increase the Hall voltage. The gain of the 67 Hertz signal would have to be decreased by the filter since the offset voltage would also be increased. The 7 Hertz distortion signal produced by the junction FET should not increase above the noise voltage when the offset voltage is increased.

3) The band-width of the filter may be decreased. This, however, would result in only slight improvement and would require highly stable a.c. electric and magnetic field frequencies.

4) The oscilloscope may be phase locked so that it is always triggered at the same phase of the 7 Hertz Hall signal. This would help in distinguishing the Hall voltage from the noise voltage.

5) An amplifier should be constructed to measure the voltage between the conductivity contacts on the sample. The sample voltage used in calculating the mobility was that of the voltage applied at the sample voltage contacts. Little error resulted from doing this as the gold contacts were of relatively low resistance.

Although the silver oxide films produced in the high vacuum unit decomposed slowly with time, they were quite stable with little drifting of the offset voltage. Since the films did not decompose more quickly while being heated, it would be possible to measure the Hall voltage versus temperature. A thin cryostat to be placed between the poles of the magnet would have to be constructed, using non-metallic materials in order to avoid eddy currents.

It is felt that the films sputtered with a substrate temperature of -60°C to -40°C were initially silver peroxide (AgO). Annealing of the films at room temperature resulted in the resistance decreasing ($\rho = 10^2$ ohm-cm). The films then started to decompose, producing oxygen vacancies in the AgO crystal structure (n-type conduction). Further decomposition and annealing resulted in the gradual formation of the Ag_2O crystal structure with interstitial oxygen atoms (p-type conduction). Additional decomposition formed intrinsic Ag_2O with a resistance of 10^{11} ohms ($\rho = 10^7$ ohm-cm).

This was followed by its rapid decomposition caused by the catalytic action of excess silver atoms. The band gap of AgO thus has a value of 0.31 eV. The band gap of Ag₂O as measured by other researchers has a value of approximately 1.4 eV. A band gap value somewhere between these two will thus be measured as the film changes from AgO to Ag₂O.

The low value of the mobility of 0.1 cm²/volt-sec. is probably due to such factors as the polycrystalline status of the film and thin film effects.

BIBLIOGRAPHY

1. Putley, E.H. - The Hall Effect and Related Phenomena -
(Butterworths).
2. Suzuki, T. - Zeitschrift fur Naturforschung 12a pp 497-499 (1957).
3. Rollins, T.L. - Thesis : Some Properties of Silver Oxide Films -
July, 1965 - Department of Physics - University of Alberta.
4. Liebermann, M.L. and Medrud, R.C. - Journal of Electrochemical
Society 116 pp 242-247 (1969).
5. Keyes, F.G. and Hara, H. - Journal of the American Chemical
Society 44 pp 479-485 (1922).
6. Perny, P.G. ; Laville-Saint-Martin, B. ; Roesler, P. and Haller, B.
- Journal de Physique et la Radium 25 pp 5-11 (1964).
7. Gross, E.F. and Kreingold, F.I. - Optics and Spectroscopy 10
pp 211 (1961).
8. Bell, A.G. and Venning, B.H. - Journal of Scientific Instruments 40
pp 239-243 (1963)

Appendix I : Cathodic Sputtering

Cathodic or diode sputtering takes place in plasma. When a high (1 to 2 kV) voltage is applied between two plates under partial vacuum such that they are separated by about one and a half to five or more times the mean free path of the electrons, a current of electrons and ions will flow between the two plates. The electrons are accelerated towards the positive plate (anode), colliding with atoms of the gas and producing positive ions and other electrons. These ions are accelerated towards and strike the negative plate (cathode). Because of their high momenta the ions knock out (or sputter) the atoms in the cathode. These sputtered atoms diffuse through the plasma with some settling on the anode. If the sputtered atoms react with the energized gas molecules of the plasma and form a chemical compound when they settle on a surface, the process is referred to as reactive diode sputtering.

Appendix II : Temperature Difference Across the
Glass Slide while Sputtering

Prior to measuring the slide temperature at the top of the slide, an estimation of the temperature difference across the glass slide was necessary.

Sputtering conditions were 1500 V and 10 mA (0.25 mA/cm^2). The power consumption was 0.375 watt/cm^2 . Since about a quarter of the total power is dissipated in the glass slide, the energy U falling on the bottom of the glass slide was 0.67 watt/cm^2 ($0.016 \text{ cal/sec. cm}^2$).

The thermal conductivity equation is :

$$U = - \frac{K \Delta T}{d} \quad (\text{II-1})$$

where K - thermal conductivity (of glass = $2 \times 10^{-3} \text{ cal/cm sec } ^\circ\text{C}$)

ΔT - temperature difference ($^\circ\text{C}$)

d - distance over which ΔT exists (cm)

For a glass slide thickness d of 0.118 cm, the temperature difference is found to be 0.9°C , i.e. only a small loss of accuracy would occur by measuring the temperature at the top of the glass slide.

<u>OAI</u>		<u>OAI</u>
150K	Input Impedance	150K
10K	Output Impedance	50 Ω
15 K Hz.	Bandwidth	15 K Hz.
1500-2000	Gain	1500-2000
200:1	C.M.R.R.	20,000:1

B29989